MICROCOPY RESOLUTION TEST CHART

NATIONAL BUREAU OF STANDARDS-1963-A

REPORT DOCUMENTATION PAGE	READ INSTRUCTIONS BEFORE COMPLETING FORM

1. REPORT NUMBER	2. GOVT ACCESSION NO.	3. RECIPIENT'S CATALOG NUMBER
ONR-CR-215-245-1		

4. TITLE (and Subtitle)	5. TYPE OF REPORT & PERIOD COVERED
ADVANCED FAULT DETECTION AND ISOLATION METHODS FOR AIRCRAFT TURBINE ENGINES .	ENGINEERING TECHNICAL REPORT. 1 Jan 76-1 May 77.
	6. PERFORMING ORG. REPORT NUMBER

7. AUTHOR(s)	8. CONTRACT OR GRANT NUMBER(s)
R.L. De Hoff W.E. Hall	N00014-76-C-0420

9. PERFORMING ORGANIZATION NAME AND ADDRESS	10. PROGRAM ELEMENT, PROJECT, TASK AREA & WORK UNIT NUMBERS
Systems Control, Inc. (Vt) 1801 Page Mill Road Palo Alto, CA 94304	5415

11. CONTROLLING OFFICE NAME AND ADDRESS	12. REPORT DATE
Office of Naval Research 800 North Quincy Road Arlington, VA 22217	February 1978
	13. NUMBER OF PAGES
	101

14. MONITORING AGENCY NAME & ADDRESS(If different from Controlling Office)	15. SECURITY CLASS. (of this report)
SAME	UNCLASSIFIED
	15a. DECLASSIFICATION/DOWNGRADING SCHEDULE

16. DISTRIBUTION STATEMENT (of this Report)

Distribution of this document is unlimited.

17. DISTRIBUTION STATEMENT (of the abstract entered in Block 20, if different from Report)

D D C

SEP 19 1978

F

18. SUPPLEMENTARY NOTES

19. KEY WORDS (Continue on reverse side if necessary and identify by block number)

Engine Diagnostic Systems
Fault Detection
Engine Performance Monitoring
Engine Trending

20. ABSTRACT (Continue on reverse side if necessary and identify by block number)

Aircraft engine diagnostic methods are reviewed. The role of computer-aided diagnostic procedures for current and future engines is discussed from the aspects of performance monitoring, trending, and fault detection/isolation. Development of advanced maximum likelihood or regression algorithms for each of these is presented. A methodology is developed for applying these algorithms to models derived from engine test stand or flight data. Specific computational results are given for a high performance turbofan engine.

TABLE OF CONTENTS

TABLE OF CONTENTS (Continued)

LIST OF FIGURES

LIST OF TABLES

SECTION I
INTRODUCTION AND SUMMARY

1.1 INTRODUCTION

The increasing performance of advanced aircraft engines, such as the existing F-15/F-16 F100 turbofan and the projected variable geometry engines for future Navy V/STOL aircraft, places complex requirements on engine fault diagnosis and performance monitoring. Such requirements can best be met by the efficient utilization of engine sensors and on-board or off-board computer processing.

There are three principal categories of fault detection and isolation which are useful for discussing the computational architecture of the required algorithms to achieve this diagnostic objective. These are:

(1) <u>Dynamic flight-critical fault detection/isolation</u> for monitoring of sudden failures of sensors or engine components (e.g. FTIT, N1, N2 sensors).

(2) <u>On-line isolation of non-flight-critical faults</u> for monitoring of status of a single aircraft's engine component performance over a single flight or intermaintenance period.

(3) <u>Off-board trending of data</u> for monitoring status of an aircraft engine over extended periods to determine necessary logistical maintenance requirements.

This document summarizes the various aspects of engine performance monitoring and how advanced system identification technology can be applied, to provide a true state-of-the-art engine diagnostic system which is readily transferred to developmental and operational phases.

Engine performance monitoring techniques have long been applied to aircraft turbine engines. The procedures were initially restricted to manual ground trims of the hydromechanical governor to account for engine deterioration and aging effects. The imprecision of this manual technique, due to the complexity of engine performance measurement (even on the ground) lead to reduced engine life and short overhaul periods for certification.

Two other problems arise when the technique is applied to real engines. Sensor characteristics are typically worse in the installed environment over the engine lifetime scale than specified by manufacturers. Most of these effects are due to two-dimensional flow characteristics of the gas stream and to unmodeled disturbances on the measurements. Sensor errors are also typically not white and are correlated with engine performance degradation. With the advent of modern twin-spool turbofan engines and their high performance requirements, the engine trim, fault detection, and maintenance scheduling problems have quickly saturated the capabilities of ground-based evaluation procedures and are currently the largest contributor to engine lifecycle costs.

Briefly stated, the performance monitoring problem attempts to measure small variations in many parameters with poorly repeatable sensors in a time-varying environment. Numerical techniques are available to utilize the measurements to produce accurate engine status information for both fault detection and performance monitoring. By utilizing digital processing of engine data, engine overhauls can be limited to appropriately degraded engines and to sufficiently deteriorated components yielding significantly improved in-service performance and higher maintenance efficiency.

1.2 SUMMARY

The report discusses the initial development of a comprehensive fault diagnostic - performance monitoring system methodology based on a generalized system identification formulation [1]. An approach to the problem of on-board and off-board processing of flight-acquired data is specifically addressed for an advanced multicomponent engine - the F100 turbofan engine. The algorithm development and validation techniques are described which are compatible with data protocols of the U.S. Air Force Engine Diagnostic System (EDS) development program currently in progress for the F-15/F-16 aircraft propulsion system.

This report is organized as follows:

- Section II - Engine Monitoring Techniques

    This section represents an extensive review of fault diagnosis and performance monitoring literature over the past 30 years. An attempt is made to organize the approaches to the problem within a general framework of statistical data analysis. Several current systems are discussed in detail.

- Section III - Methods in Performance Monitoring, Trending, and Transient Fault Detection

    This section describes an approach to the problem of monitoring critical engine parameters utilizing imperfect sensed parameters in the engine. The development and evaluation of generic engine models are described. Algorithms are discussed for processing measurements and estimating parameter values.

- Section IV - Performance Monitoring for the F100 Turbofan Engine

    Preliminary results are presented in this section. Model development for a generic F100 system of equations is described which can be applied to acquired data.

- Section V - Summary and Conclusion

    This section presents the important initial conclusions of the study. A brief description of the specific application to the F100 is included.

3

SECTION II
ENGINE MONITORING TECHNIQUES

2.1 INTRODUCTION

The modern aircraft engine probably represents the most complex interaction of mechanical, aerodynamic, thermodynamic, and electronic phenomena in any vehicular subsystem. It is critical to aircraft missions to maintain a high level of durability and reliability. Near future propulsion system configuration requirements, however, are specifying significant deviations from the engines flown over the past decade, including multi-component interconnections and variable geometry [2]. For present and future aircraft, electronic data acquisition and control systems will be required to integrate previously isolated functions including diagnostic and monitoring procedures currently practiced on modern propulsion plants [3]. Techniques for utilization of this advanced capability are currently untested in an operational environment. Also, no single diagnostic or monitoring procedure has been accepted for any engine application. In this section, a historical summary of engine monitoring, and a synopsis of modern engine analysis procedures are presented.

2.2 HISTORICAL PERSPECTIVE

Aircraft engine monitoring began in early commercial piston service in the 1930's over long haul routes. Temperature and torque were monitored by the flight crew periodically and consistent changes were flagged for investigation [4]. The examination of the temporal relationships between engine parameters was called trending and, in one form or another, is still a practiced procedure

5

today. Systematic engine monitoring requirements were relaxed as piston engines became more reliable and powerful and route times became shorter. A strong resurgence occurred when the first turbine engines entered into commercial service [4]. Unlike piston engines, aircraft turbines utilize direct aerodynamic to mechanical energy conversion which can be significantly affected by small changes in component configuration [5].

In the early 1960's, electronic data acquisition techniques, mostly analog, were combined into the first of many on-board engine monitoring systems in Project EASY [6]. Many of the problems inherent in a practical electronic system were uncovered during this project and no implemented system resulted.

Data processing and sensor technology has radically changed since that time. Most major aircraft systems have developed, at least initially, an automated data acquisition system for engine monitoring [7,8,9]. Many new approaches have been proposed and many revised. Experience has shown that successful systems must be tailored to the aircraft mission, and maintenance environment [9].

2.3 CURRENT SYSTEMS

Three military monitoring systems represent the practical, state-of-the-art approach to engine fault detection within a maintenance environment. The approaches of these systems are briefly reviewed in Sections 2.3.1 through 2.3.3. A commercial system is discussed in Section 2.3.4.

2.3.1 In-Flight Engine Condition Monitoring System (IECMS) [10,11]

IECMS is an in-flight condition monitoring system installed on the TF41 engines in the VSD A7-E aircraft. The system utilizes engine and airframe sensors and a digital processing unit to

6

determine engine component failures. Data of abnormal events is stored on a tape cassette for further, ground-based processing. The system measures both engine and control parameters and monitors discrete inputs from the various subcomponents.

The organization of the system is functionally separated into eight modes of operation. Depending on the mode, events are monitored which can indicate abnormal conditions. Fault accommodation for several common control failure modes (primarily sensor failures) is provided using analytical redundancy. Performance is monitored by checking values of fuel flow against rotor speed and ambient conditions. No historical data is used. This type of calculation is often referred to as "snapshot." Measurements utilize temperature, pressure, flow, vibration and stroke for input to modularized algorithms.

Initially, the IECMS was flight tested for validation. Verification of each detected event by on-sight engineering personnel was required by a high false alarm rate (initially over 100%). An 85% accuracy figure was achieved on the manually verified alarms in this test. A carrier deployment was undertaken to test the impact on the system in an operational environment. The false alarm rate decreased during the test phase (to under 3%); however, nearly as much maintenance effort was required to support the electronic system as was required to maintain the engines. The maintenance man hour per flight hour (MMH/FH) was below fleet average for both the IECMS support aircraft and the standard control group [12]. Thus, no conclusion can be presently drawn concerning the impact of IECMS on maintenance costs.

2.3.2 Automated Inspection Diagnostic and Prognostic System (AIDAPS) [12,13]

AIDAPS is a U.S. Army program to develop a diagnostic system for Army aircraft. The UH-1H helicopter was utilized as the initial test bed for the system. Unlike IECMS, a significant

amount of development and testing was performed prior to deploy-
ment of a system. The AIDAPS system monitors avionics, propul-
sion, and transmission systems on the helicopter. During the
test development, degraded and failed components were inserted
in the system and the system responses were evaluated. After
the system was developed, a zero false alarm rate was initially
validated over a two-month test period. Table 2.1 shows the
overall AIDAPS test scores for implanted faults. After the
test bed development, a 1128-hour flight test program was
accomplished. The engine fault detection portion of the system,
using both vibration and gas path analysis, resulted in fewer
detections than the gear box monitoring system [14]. One strong
conclusion throughout the test was that consistency of results
between laboratory models, test cell data, and aircraft is a
function of the monitoring technique.

2.3.3 Advanced Diagnostic Engine Monitoring System (ADEMS) [15]

The ADEMS is a subsystem of the C-5A Malfunction Detection
Analysis Recording Subsystem (MADARS) which monitors over 800

Table 2.1
AIDAPS Test Results [12]

PROCEDURE	COMPONENT	FAULTS DETECTABLE	UNDETECTABLE	NOT SCORED	FALSE ALARM	TOTAL SCORED	PERCENTAGE
Vibration Monitoring	Engine	24	7	6	3	31	77.4
	Transmission	34	4	16	2	38	89.5
	HGB 4	13	0	3	3	13	100.0
	42° GB	33	0	14	2	33	100.0
	90° GB	18	14	4	1	32	56.3
Subtotal		122	25	43	11	147	83.0
Gaspath Monitoring	Compressor	7	2	5	0	9	77.8
	Turbine	6	6	8	0	12	50.0
	Combustor	1	0	0	0	1	100.0
Subtotal		14	8	13	0	22	63.7
TOTAL		136	33	56	11	169	80.5

airframe/engine (TF39) parameters. Approximately 28 engine para-
meters (per engine) are monitored in flight. Magnetic tape
recordings are produced when selected thresholds are exceeded or
when the system is given a record command. The tape recorded
data is processed at the Maintenance Analysis and Structural
Integrity Information System (MASIIS) facility at the Oklahoma
City Logistics Center. At the present time, a significant portion
of the data is not used due to the large volume and absence of
maintenance concepts geared to the outputs.

2.3.4 Commercial Programs

In-flight engine monitoring in the commercial fleet has been
used since the early 1960's. The emphasis of such systems is on
data acquisition and post-flight processing of trend data
to schedule activities [16]. The Airborne Integrated Data
System (AIDS) is a nearly standardized logic for acquisition of
engine and aircraft data [7]. Various airlines in the U.S. and
Europe have used this system for engine performance monitoring.

KSSU, the European aircraft consortium, utilization of AIDS
is a recent example of the approach used by commercial airlines.
Additional monitoring transducers specifically for DC-10 or 747
engine application were discouraged. A strong emphasis on sensor
repeatability was placed in the instrumentation specifications.

Domestic airline engine monitoring has been directed toward
long-term trending. In general, the philosophy has been to
trend-corrected engine variables in stabilized cruise. Then,
when exceedances are encountered (e.g. in fuel flow or EGT),
an engine removal and turbine overhaul is scheduled. Experience,
however, has shown that significant amounts of compressor and fan
degradation occur [5,17] which is unaffected by turbine renovation.
Test programs are currently underway to evaluate instrumentation
required for in-flight and test cell determination of engine per-
formance on a module basis.

9

2.4 ENGINE MONITORING TECHNIQUES

Many techniques for inferring engine status or change in engine status have been proposed and/or applied to various engine configurations with varying success. The major types are reviewed below.

2.4.1 Vibration Monitoring [14,18,19]

A critical area of concern in turbine engine operation is the status of the rotor support bearings and auxiliary power/free turbine transmission systems. Wear in this type of rotating part is apt to occur steadily after the appearance of an initial pit or dent. Each time this fault contacts another surface (e.g. bearing race or gear tooth), an impulse is transmitted to the structure which can be detected by various force-sensing tranducers such as piezoelectric accelerometers.

The impulse transmitted to the structure will occur at harmonic frequencies of the rotational speed of the rotor. Thus, typical vibration sensor systems utilize tracking bandpass filters to monitor vibration energy at the key harmonic frequencies [19]. The signals are often integrated for a fixed time and the vibration amplitude value sampled.

Generally, this type of system is useful to detect incipient faults in mechanical systems which have bearing or gear defects which have progressed to the failure point. Earlier flaws will not produce adequate energy to be detected over the background bearing or gear mesh noise levels. A new technique has recently been suggested which appears to produce far superior results in test bed experiments [14]. Briefly, when a gear or bearing flaw impacts the structure, a broad band energy pulse is transmitted. This results in high frequency vibration components being amplitude-modulated by the impulse. The new system high pass filters the accelerometer inputs to eliminate lower frequency

.

10

rotor harmonics and then amplitude-demodulates the resulting signal. This procedure has been shown to be sensitive to developing flaws.

2.4.2 Usage Measures [20, 21, 22, 23]

Engine aging depends on the running time and is accelerated at high temperatures. Cyclic power level excursions result in temperature changes in rotating parts and have a predominant relationship to the remaining life of the part. These facts have been incorporated into two engine life figures called low cycle fatigue (LCF) and hot section factors (HSF) [23].

LCF counts measure power excursions from lower power levels to higher power levels. During this type of "cycle," the engine hot section is subjected to stress from rotational accelerations and temperature gradients. These cycle counts are used as an age measure for the various components of the engine and in modular engines, the cycle counts are tabulated for a number of parts. When the counts exceed the limit for a part, maintenance action is required. This procedure is quite attractive in its simplicity and applicability to modular engines. It requires accurate data recording and accounting at many logistical levels. Also, the limiting LCF counts for each part are extremely difficult to determine. Setting lower limits is a conservative decision which results in higher maintenance overhead.

Hot section factor or hot time measures the exposure of the engine, primarily the turbine, to inlet gas temperatures above certain levels. This measure is then correlated with turbine wear using Advanced Mission Testing (AMT) results [21] and HSF limits are specified to determine maintenance action. This procedure is convenient and compatible with the newer AMT philosophy being employed on current propulsion systems. The trade off between conservative specification and maintenance overhead remains.

11

2.4.3 Oil Analysis [24, 25]

Oil analysis techniques can be categorized as spectrographic or particle detection. Spectrographic oil analysis determines the metallurgical composition of the engine oil. Changes in oil contaminant composition indicate predominant areas of wear. Levels indicate the amount of wear present. These procedures are accurate for particle sizes less than 2 microns, but require sophisticated laboratory equipment. Two problems are the delay in processing the analysis at a central location and detection of wear particles larger than 2 microns.

Oil chip detectors indicate the amount of metal in the oil Magnetic detectors, pressure drop switches, and light scattering devices have been used with varying degrees of success [25]. Problems occur due to viscosity changes in the oil, oil aging, and component fouling. After there is an abnormal indication, isolation to the specific faulty component may be difficult. These indicators usually provide a discrete indication of a problem rather than a continuous status level which could be used for prognostication.

2.4.4 Charged Particle Probes [25, 26]

Electrostatic probes may be placed in the engine exhaust to detect charged metal particles caused by component wear. These devices can detect incipient engine failure by measuring increases in charged particle levels which occur prior to failure. The electronics associated with the system have been proven compatible with installation in an operational environment.

2.5 THERMODYNAMIC ANALYSIS PROCEDURES [27, 28, 29]

The aircraft turbine engine has the advantage over other types of propulsion systems in that the physical phenomena can be modeled by equilibrium thermodynamic equations. Using some

mildly restrictive assumptions, the actual performance of each component in the gas path can be analytically described in steady state terms.

Analytical prediction of turbine engine performance was first attempted in an engine monitoring system around 1963 [6]. As computational techniques have improved and data acquisition and testing procedures have become more accurate, the feasibility of this approach has increased dramatically.

Thermodynamic analysis methods use analytical models to diagnose changes in component performance which may be linked to degradation, aging, or incipient failure. These procedures should be contrasted with engine measurement monitoring which tracks rotor speeds, temperatures, etc. to determine overall changes in engine performance.

2.5.1 General Framework

The general gas path analysis problem can be formulated as follows:

$$0 = f(x,u,\theta) \tag{2.1}$$

$$y = h(x,u,\theta) + v(t) \tag{2.2}$$

where x and u are vectors of engine variables and inputs are chosen for convenience in the model. θ is the vector of engine paremeters. $f(x,u,\theta)$ is the model of the engine, y is the group of sensor measurements which are related to the states and controls by $h(x,u,\theta)$ and certain random errors, $v(t)$. All gas path analysis techniques can be written as special cases of Eq. (2.1) and (2.2) using a group of lumped parameter modeling assumptions [6].

In general, Eqs. (2.1) and (2.2) are difficult to accurately formulate and solve. Usually, a redundant set of equations is obtained so that engine parameter values and sensor errors can be calculated. For example, a linearized procedure which uses corrected variables as the engine model and small parameter variations as linearization variables has been applied to engine testing in sea level static tests [25].

2.5.2 Approaches to the Problem

Two approaches to the problem formulation have been proposed in current systems and two methods of data analysis are possible. These procedures are reviewed below.

There are two data processing procedures. In the snapshot method, a model and parameters are chosen with which, given a single set of engine measurements, a set of engine and sensor parameters can be determined. Data scatter can cause a significant degradation in the results. Often, closely averaged measurements are used to reduce the scatter. This will not generally alleviate the problem as will be discussed in Section III. The advantage of this procedure is that old data does not have to be stored. False alarm rates tend to be high if simple thresholds are used.

Trending is performance analysis utilizing past data. In trending (or filtering), past data is compressed into sufficient statistics which represent information about parameter and sensor errors contained in all the measurements to date. Prognostication is possible if rates of change are estimated along with parameter values.

Two techniques are used to model the engine. In the custom baseline [30,31], a particular engine is run at various power conditions to determine the current performance. Measurements at later times reflect changes in the custom baseline and a linearization of the model is possible about the customized operating point [32, 33]. Generic baselines are analytic models

14

representing the closest approximation to the nonlinear engine build. Rather than a set of baseline numbers, the generic baseline is a set of equations which model the thermodynamics of the engine if nominal losses and efficiencies are assumed.

A custom baseline represents a historical data record. Thus, a snapshot calculation using a custom baseline is somewhat contradictory. Several systems using generic baselines and snapshot calculations have been implemented with varying success [29, 35]. In general, the requirement for simplification of the model often introduces errors exceeding the changes caused by component deterioration.

The general generic solution to Eqs. (2.1) and (2.2) and the specialization to custom baselining and snapshot calculations are described in detail in Section III.

2.5.3 Dynamical Analysis

Eq. (2.1) is a special case of the exact expression describing engine behavior in an installed environment, namely

$$\dot{x} = f(x,u,\theta,t) + w(t) \tag{2.3}$$

where $f(x,u,\theta,t)$ models the time dependence of the machine and $w(t)$ models the disturbances which invariably act on the system. Techniques have been suggested which utilize this dynamic model to monitor critical parameters in the engine [34, 36, 37]. The simple example of this type of technique is the trending of time-to-zero speed after ground shutdown [25] to monitor bearing friction on the rotor shafts.

More sophisticated procedures utilize dynamic data analysis to gain information concerning component characteristics which influence response to throttle commands or actuator changes (such as bleed flow). Introduction of the dynamics into the problem also increases the number of fault parameters. Thus, in addition

15

to lumped component efficiencies and effective areas, parameters such as spool time constants and control effectiveness are added to the overall set [34]. It is possible that these parameters are far more sensitive to degradation effects than steady state efficiencies, and as such represent more efficient fault sensitive indices.

The dynamic parameter estimation problem is a more cumbersome modeling task and data processing effort. However, with sufficient simplification, in-flight algorithms may be developed which can utilize continuous, dynamic data inputs as the basis for fault monitoring. These procedures will be discussed in Section III.

2.6 PRACTICAL ASPECTS OF THE PROBLEM

Experience over the past two decades has shown that accurate in-flight engine monitoring is an extremely difficult problem which involves engine data acquisition and transfer, real-time processing algorithms, off-board processing and reduction and incorporation within the existing maintenance procedures and logistical framework. Some of the problems of the practical system are summarized below [9, 25, 35, 38].

(1) Measurement Accuracy. Transducers measure quantities which are not averaged gas path variables. Inaccuracies arise in the sensor and along the information path to the computer. Error budgets must be observed to keep this error source from overwhelming required accuracy. Sensors themselves fail and outputs shift with sufficient regularity to cause problems in an installed system.

(2) Modeling Accuracy [25,12]. Experience has shown that modeling techniques are critical. Utilization of computer simulations must be closely correlated with test stand data. Aircraft data should be expected to differ from test stand results. Models such as generic baselines must be formulated in a way to accurately account for these effects.

16

(3) Fault/Parameter Correlation [5,21]. The most difficult
     part of the problem is determining how overall model
     parameter changes correlate with maintenance acti-
     vities such as compressor cleaning or turbine over-
     haul.

(4) Complexity of the Algorithm [30].   Algorithms to
     solve all the problems can easily exhaust the most
     extensive computer capability. Computational re-
     quirements must be balanced with computer avail-
     ability at each step in the data processing flow.
     Accuracy tradeoffs are important, also.

2.7 SUMMARY

The history of engine performance monitoring has been re-
viewed. The early efforts in turbine engine analysis were
compared with current programs in this area. Three military
programs, IECMS, ADEMS, and AIDAPS were reviewed for back-
ground and as examples of the current philosophy. Various pro-
cedures have been discussed which can be used to measure engine
health. Thermodynamic cycle monitoring or gas path analysis
has been derived in general and specific approaches of current
systems have been reviewed. Problems in the gas path analysis
have been presented which can significantly impact the useful-
ness of any algorithm.

Section III describes the equations of engine performance
analysis from a general viewpoint. The specialization to various
implementation forms is derived.

17

SECTION III

METHODS IN PERFORMANCE MONITORING, TRENDING, AND TRANSIENT FAULT DETECTION

3.1 INTRODUCTION

Performance monitoring is the utilization of regularly acquired, imperfect measurements to infer the present and future status of the system relative to a previous status or an ideal norm. Section II presented a historical review of the development of performance monitoring systems. These approaches have naturally sprung from non-parametric techniques practiced on early spark ignition and turbine engine aircraft. This section discusses the problem from a general viewpoint which includes present monitoring techniques as special cases.

Failure detection for dynamic systems is closely allied to performance monitoring [1]. In general, these procedures must make rapid inferences from flight acquired data, most often in real time. The computational capabilities of such systems using on board computers may be restricted by processing time and storage. Performance monitoring techniques are based on the same theoretical foundations as real time failure detection; however, the application and emphasis are shifted from rapid decision outputs to accurate utilization of the measurements for diagnostics and prognostication at the ground maintenance level.

With the advances in modern electronic processing capability and reliability, the distinctions between on board/off-board capability, real time and post flight analysis and thus monitoring and detection have become less pronounced. Many more complex algorithms from data analysis methodologies can now be applied in a real time environment. The time scale differences between

failure detection and performance monitoring are presented in Figure 3.1 for typical engine events. The unified problem can be viewed as a multiple time scale system. For time constants comparable to transient engine response processes, a fast decision must be made with a relatively small amount of information. These decisions involve gross changes in engine/instrumentation characteristics. This type of processing may be defined as detection. For time constants much longer than engine dynamic processes, a large amount of data is available. The changes in the system due to these events are typically quite small and performance monitoring techniques attempt to reduce the vast amount of operating data to a set of statistical measures describing the status of the system. This section will primarily emphasize performance monitoring algorithms which are adaptable to minicomputer implementation at the flight line maintenance level and compatible with flight acquired data inputs.

A general formulation of the detection/monitoring problem will be presented in Section 3.2. Various assumptions leading to a static model are presented in Section 3.3. (Section 3.3.1 systematically expands on the method of static model analysis via quasi-linearization. The actual development of mathematical models is presented in Section 3.3.2.) Trending applications are discussed in Section 3.4. Section 3.5 presents a method for utilization of transient response data to infer a different class of performance-indicating parameters.

3.2 GENERAL FORMULATION

It is fundamental to this development that fault detection and performance monitoring procedures are subsets of the parameter identification problem. In general, the turbine engine, or any system, can be mathematically described by a set of nonlinear equations (to most any degree of accuracy) as follows:

TIME TO DETECT FAULT
(SECONDS)

0.1   1.0   10   100   1000   10000

SURGE
MAIN BURNER BLOWOUT

High Power   TIT SENSOR OUT

N_1, N_2, P_B, P_6 SENSOR OUT

T_2, P_2, $T_{2.5C}$ SENSOR OUT

FUEL VALVE, VANE, STATOR, NOZZLE ACTUATOR OUT

FUEL VALVE PERFORMANCE SHIFT
FUEL DISTRIBUTION PLUG

THROWN TURBINE BLADE

SEAL LEAKAGE, DIRT, CORROSION
(FAN, COMPRESSOR, TURBINE
EFFICIENCY DEGRADATION)

TIMES DEPENDENT ON:

1. Power/Flight Condition
2. Engine Transient or S.S. Operation
3. Type of Failure
   a. Zero
   b. Full Over
   c. Last Value
4. Severity of Fault
5. Required Action
6. Data Sample Rate

Figure 3.1 Turbofan Engine Fault Detection Epochs

21

$$0 = f(\dot{x}, x, u, \theta, w) \tag{3.1}$$

where the distributed aerothermodynamic, mechanical and electrical processes are lumped into a finite state, x, representation using lumped parameter forms of the physical laws for these phenomena. States may be distinguished from controls in that time derivatives of the former elements occur. Also, for n state variables, n sets of Eq. (3.1) must be written. Controls, u, disturbances, w, and parameters, θ, are quantities which can be distinguished by measurement or manipulation. The controls are quantities which are manipulated and perhaps measured. Disturbances and parameters are usually desirable to know but not easily measured.

Measurements are taken on various quantities in the engine. These sensed parameters are related to the states, inputs and parameters according to the general algebraic expression:

$$y = h(x, u, \theta) + v(t) \tag{3.2}$$

where random errors are introduced by random unmeasurable processes.

Equations (3.1) and (3.2) are general enough to provide a starting point to define the fault detection problem relative to control design, state estimation, or other related technologies.

The engine model can be arranged in Eq. (3.1) to describe the dynamics of the system by a unique set of equations as follows:

$$\dot{x} = f(x, u, \theta, w) \tag{3.3}$$

Deterioration of engine components affects the operational characteristics of various subsystems and the entire engine. It is fundamental to the fault diagnosis objective that this deterioration, affecting the parameters, θ, of Eq. (3.3)

22

can be detected and isolated. This objective indicates that the fault detection/isolation can be treated as a parameter estimation problem. Usually, the pressures and temperatures are measured at many engine stations. Other measurements include rotor speeds, vibration level, fuel flow, etc. Isolation of faulty components using these measurements is complicated by two major considerations: (a) systematic errors in instruments (bias, scale factor errors) may appear to be degradations in engine performance, and (b) a fault or a set of faults may produce a similar effect on measurements as another fault or set of faults.

The problem of fault detection and performance monitoring can be formalized on the basis of the following assumptions:

Assumption I: Component and sensor deteriorations and failures to be observed affect the operation of the engine, control system, inlet, etc., in such a way that changes in observed quantities can be used to discriminate between the failed/unfailed sensor or the deteriorated/undeteriorated state.

Assumption II: The operation of the engine and subsystems in its healthy and unhealthy state can be modeled by equations of type (3.2) and (3.3).

Assumption III: The transformation between values of engine fault parameters, θ, and aging effects, control failure modes, mechanical defects, sensor errors and miscalibration can be established from theoretical inferences and verified by operating records or specifically designed tests.

Given assumptions I-III, the problem can be stated as follows:

For the system of equations:

$$\dot{x} = f(x, u, \theta, w) \tag{3.4}$$

$$y(k) = h[x(k), u(k), \theta] + v(k) \qquad k=1, 2, \ldots \tag{3.5}$$

determine the statistics of the unknown parameters, θ, including the mean, variance and distribution at each time given some subset of the historical data.

23

Suppose that an operating record is given representing the operation of a healthy or nominal engine at arbitrary time points as follows:

$$\{y_n(k)\} \qquad\qquad k = 1,\ldots,N \qquad (3.6)$$

Suppose another operating record is supplied for another engine which has the same values of input variables representing an off-nominal engine with degradation, component aging, sensor inaccuracies and failures present. These may be written as follows:

$$\{y(k)\} \qquad\qquad k = 1,\ldots,N \qquad (3.7)$$

The difference between the two outputs can be written as follows:

$$\Delta y(k) = y(k) - y_n(k) \qquad\qquad (3.8)$$

$$= h[x(k),u(k),\theta] - h[x_n(k),u(k),\theta_n] + v(k) \qquad (3.9)$$

The difference can be expanded in terms of small values of the parameter differences. This linearization step [33, 38] is performed even if a nonlinear model is assumed and numerical minimization is used. The resulting form is given below:

$$\Delta y(k) = \left(\frac{\partial h}{\partial x(k)} \frac{\partial x(k)}{\partial \theta} + \frac{\partial h}{\partial \theta}\right) \Delta\theta + v(k) \qquad (3.10)$$

$$\frac{d}{dt} \frac{\partial x}{\partial \theta} = \frac{\partial f}{\partial x} \frac{\partial x}{\partial \theta} + \frac{\partial f}{\partial \theta} \qquad (3.11)$$

The parameter estimation problem is to find the $\Delta\theta$ vector which accomplishes the following optimization

$$\hat{\theta} = \max_{\theta \varepsilon \Theta} J(\theta|Z) \qquad (3.12)$$

24

where the objective function, J, is formulated to maximize the likelihood of the estimate, minimize the cost of an error, etc., depending on the preferences of the analyst.

Two approaches to the problem become evident at this point. The generic or nominal baseline approach uses a form of measurement sequence, Eq. (3.6), which is the output of a detailed simulation or model of the engine at nominal values of the build parameters. The custom baseline approach uses an output record actually measured or created from averaged measurements of the particular engine being observed. The differences in the two approaches are more practical than theoretical since linearized behavior is assumed in both cases. In the following discussions, the differences in the resulting algorithms will be identified.

3.3 FAULT MONITORING ASSUMING STATIC MODELS

Most engine performance monitoring techniques which utilize thermodynamic principles assume the engine and aircraft are operating in a steady state condition (e.g., static). This approach is often called gas path analysis. The thermodynamic laws governing engine behavior can be written in simpler terms than the equations modeling unsteady aerodynamics, heat transfer or torque balance phenomena. However, since the engine, particularly in flight, is never completely static, errors will occur due to these temporal effects.

Under the assumptions of static behavior, Eq. (3.3) may be written as follows:

$$0 = f(x, u, w, \theta) \tag{3.13}$$

The measurement equation containing all systematic uncertainties is repeated below:

$$y = h(x, u, \phi) + v \tag{3.14}$$

25

There have been many approaches to the performance monitoring problem as discussed in Section II. Certainly, the complexity of the propulsion system and availability of data acquisition and processing capability have a strong impact on the sophistication of the procedure [39]. The mathematical approaches to performance monitoring previously developed for jet engines are reviewed below and put in the context and symbology of parameter identification.

There are two types of engine monitoring and fault detection. They may be called direct trending and inferential methods. Direct trending is the original procedure for tracking important engine measurements and noting changes. Inferential methods attempt to use changes to infer the cause of the change. These two approaches will be discussed below.

Direct trending [10,15] methods are performed by many automated data recording systems. Engine measurements such as rotor speeds, fuel flow, EGT, and EPR are recorded and corrected to standard conditions. These measurements are taken at a constant power condition and flight point so that, if the engine remains healthy, the measurements should be constant. If the measurements change over time, it is an indication of a change in engine operation or sensor effects. Fault isolation is performed by associating a "direction matrix" with the measurements. The sign of the parameter changes for each measurement change is noted. A table is created which relates typical engine failures to the directions of measurement changes and this is used as the isolation technique.

This approach requires repeatable operating conditions for the aircraft. It's application has been predominenatly in the commercial environment where a stabilized cruise is common. Unfortunately, there are more engine and sensor faults than can be uniquely associated with measurement changes so that the "direction matrix" often has several possibilities for each entry.

26

Inferential techniques use quantitative measurement changes and a model of engine performance to analytically infer the cause and magnitude of the set of deterioration parameters.

Direct analytical modeling [29,41,42] uses a simplified work and energy relationship to establish nonlinear, algebraic relationships between gas path quantities. In this case, fault parameters, e.g., lumped efficiencies, area changes, pressure drops, are analytically derived as a function of measured quantities, e.g.,

$$\eta_c = K \frac{P_{rc}^{\gamma-1/\gamma} - 1}{T_{rc} - 1} \qquad (3.19)$$

where the compression pressure and temperature ratios, P_{rc}, T_{rc}, are measured. The fault parameters are monitored and trended. When large deviations occur, failures are expected. When smaller consistent trends are detected, deterioration may be involved. Practical problems arise in this situation, e.g., multiple faults, sensor calibration drift, modeling errors, sensor flow errors which are influenced by age, variable geometry effects, etc. However, with reasonably simple gas paths, these techniques have been experimentally demonstrated.

The second category of inferential methods includes linear or quasi-linear approaches. These procedures have shown promise in actual development programs and in several prototype engine analyzers [28,30,32].

One procedure [27,28] utilizes a numerical approach for direct calculation of fault parameters:

$$\Delta y = y - f(x) \qquad (3.23)$$

$$\underline{\Delta \theta} = Q \ \underline{\Delta y} \qquad (3.24)$$

27

Here, deviations from the custom baselines, $f(x)$, are measured. This baseline is calculated as a function of a single corrected variable, x, from installed or test stand data. The fault coefficient matrix, Q, is analytically [47] derived for a particular flight point. The number of measurements and parameters are assumed equal, the custom baseline is assumed to be a function of a single variable and the relationship

$$\underline{\Delta y} = P \ \underline{\Delta \theta} \tag{3.25}$$

is assumed calculable and invertible. This procedure is more applicable to land-based turbine operations because of the assumptions concerning univariate baselines, constant fault coefficient matrices, etc. Procedures [30,39] for choosing fault parameters and measurements to give the most accuracy have not been systematically developed. A more sophisticated technique is shown below:

$$\Delta y_i = y_i - f_i(y_j) \qquad\qquad i=1,\ldots,p \tag{3.26}$$

$$\underline{\Delta y} = P(y_j) \ \underline{\Delta \theta} \tag{3.27}$$

$$\underline{\Delta \theta} = Q(y_j) \ \Delta \underline{y}$$

$$Q = (P^T W P)^{-1} P^T W \tag{3.29}$$

This procedure [30] is an extension of the first approach using a more accurate data processing approach. A set of measurements, $\underline{y}$, includes data with some random uncertainty. A deviation is calculated from a custom baseline measured by a single abscissa value, y_j (e.g., corrected speed). These baselines can be shifted or biased by additional ambient variables (e.g., Mach no.) to account for some altitude effects which are not easily modeled by standard nondimensionalization. Similarly, the fault coefficient matrix is developed at a number of operating points and the

28

elements are mapped by a scheduling variable, y_j. More measurements than parameters are taken and a weighted, least squares solution is obtained. The choice of measurements and parameters can be accomplished with a specialization of the technique discussed in Section 3.4.

The linearization procedures have had the most practical success because the deviations of parameters between new and deteriorated engines (especially for high performance systems) is small. While this fact justifies the linearization, it complicates the modeling and measurement problem significantly. In particular, while it is far more economical to use simulations of engine deterioration to calculate baselines and fault derivatives, accuracy limitations between actual engine and simulated behavior can produce anomalous results unless compensated for in the processing of the data.

There are three important considerations in the application of this method. Since custom baselines are measured, practical engine test limitations specify a univariate baseline function (e.g., determined by power lever angle, corrected speed, etc.). Since variable geometry engines have more degrees of freedom, these must be reduced to a single degree of freedom problem using: (1) corrections of variables to standard day conditions, (2) utilization of control schedules to resolve geometry position ambiguity, and (3) neglecting unmeasurable random disturbances such as bleed rates and seal leakages. This scheme is often complicated by modern control logic which "uptrims" engine response to compensate for component deterioration. Also, errors in measuring baseline performance, set point variables (abscissae) and ambient conditions degrade the starting point for performance monitoring. The second important consideration is altitude and nonstandard day effects. For small pressure ranges and large temperature variations, scaling laws (for fixed geometry) can be applied to the turbine to correct changes due to operating conditions scaled by temperature and pressure. At altitude and nonzero flight speed, Reynold's number, Mach number and

29

radial flow effects such as distortion and burner effects tend to significantly reduce the applicability of the scaling relationship. This restricts the operating envelope of the diagnostic program to take-off/landing conditions or the models used in Eqs. (3.26)-(3.29) become extremely complex.

The third consideration is instrument errors which change slowly, change after maintenance and are related to the power or flight condition [44,45]. All of these effects tend to cause deviations in derived parameters, $\Delta\theta$, which can mask the small effects expected due to deterioration and aging. Effects of instrument deterioration on parameter estimation accuracy are presented in Ref. 1.

These three potential effects tend to limit the accuracy of multiple fault diagnostic approaches. A general formulation is presented which utilizes more sophisticated filtering techniques to extract the maximum information (in a statistical sense) from the measurements.

3.3.1 Quasi-Linearization Method

Returning to the general set of equilibrium conditions of the engine written in Eq. (3.13):

$$0 = f(x, u, \theta, w) \quad , \tag{3.30}$$

it is possible to assume that the performance parameters, θ, and unknown disturbances are small when compared to effects of primary variables such as fuel flow or rotor speeds. In this case, the equations can be linearized as follows:

$$0 = f_o(x,u) + f_\theta(x,u)\delta\theta + f_w(x,u)\delta w \tag{3.31}$$

where

$$f_o = f(x,u,\theta_o,w_o) \tag{3.32}$$

$$f_\theta = \left. \frac{\partial f(x,u,\theta,w_o)}{\partial \theta} \right|_{\theta = \theta_o} \tag{3.33}$$

$$f_w = \left. \frac{\partial f(x,u,\theta_o,w)}{\partial w} \right|_{w = w_o} \tag{3.34}$$

The nominal values of deterioration parameters and disturbances are determined from examination of many engine builds. The deviations $\delta\theta$ and δw specify the amount each parameter and disturbance differ from the nominal.

The modeling requirements for states, control variables, parameters and disturbances can be made more exact at this point. Equation (3.31) represents n algebraic equations describing the equilibrium state. The engine has m independent degrees of freedom in steady state corresponding to the number of free or independent input and control variables. The excess number of equations, $n-m$, represents equality constraints on the state variables. The state variables themselves do not necessarily maintain any dynamic identification since the problem has been reduced to an algebraic solution. Thus, "state" variables may be chosen for convenience, in this case, to represent measured quantities. Equation (3.31) can be represented as a quasi-linear regression model which relates measured variables to control inputs, other measured variables, and parameters, as follows:

$$x = g_o(x,u) + g_\theta(x,u)\delta\theta + g_w(x,u)\delta w \tag{3.35}$$

The selection of the form of Eq. (3.35) is permitted only when static behavior is assumed. The "model" shows that the quantities, x, are related to a nominal or <u>generic</u> engine baseline, $g_o(x,w)$, which is a function conveniently represented by a group of other state and control variables. The exact value attained by x is also influenced linearly by engine

31

performance parameters, $\delta\theta$, and unknown and random disturbances, δw. The state is defined as the ideal value which would be measured in the perfect, nonlinear engine model which included all effects accurately simulated. Of course, the "true" state cannot be measured on any real engine. The relationship between generic engine behavior and measured engine performance is the inferential problem posed by performance monitoring.

It is assumed that measurements of x are taken with transducers whose outputs can be modeled as follows:

$$y = x + g_\phi(x,u)\delta\phi + v \qquad (3.36)$$

where $v(t)$ is a zero mean, random process modeling temporally varying errors in the static measurement which include channel noise, high frequency processes, and engine disequilibrium. The measurement function, $g_\phi(x,u)$, represents systematic errors in the measurements which could include bias offsets, scale factor effects, radial flow effects (e.g., pressure gradients), and cross couplings (e.g., temperature effects on scale factor). The modeling requirements and restrictions on $g_\phi(x,u)$ will be discussed in Section 3.5.

The models in Eqs. (3.35) and (3.36) can be reduced to a more convenient form appropriate for parameter estimation. Substituting Eqs. (3.35) and (3.36) yields the following

$$y - g_0(x,u) = g_\theta(x,u)\delta\theta + g_\phi(\dot{x},u)\delta\phi + g_w(x,u)\delta w + v$$
$$(3.37)$$

which is a standard form for quasi-linear estimation using least squares or maximum likelihood methods. However, in the case of Eq. (3.37), the n equations are written in terms of redundant sets of independent variables (x,u) which are only approximately measured. The models are constructed in this manner (see Section IV) to take advantage of simple relationships among measured variables in the engine.

To account for the uncertainty in x and u, a two-step procedure can be used to estimate the parameters. The algorithm is discussed below.

An initial estimate of the parameter values is made using results of previous data or ad hoc assumptions. A group of measurements is processed together and reduced to an updated set of parameter values which reflect the best estimate of engine status and instrumentation errors. For a group of N inputs, $(u(i),i=1,N)$, the implicit equations, Eq. (3.35), are numerically solved for x, yielding the following result

$$\hat{x}(i) = g_o(\hat{x}(i),u(i)) + g_\theta(\hat{x}(i),u(i))\hat{\theta}(0) \qquad (3.38)$$

The points, $\hat{x}(i)$, represent the best estimate of the engine state without incorporating the new data but at the operating conditions where the new data is taken. The measurement equation is written:

$$\hat{y}(i) = \hat{x}(i) + h_\phi(\hat{x}(i),u(i))\hat{\phi}(0) \qquad (3.40)$$

where $\hat{y}(i)$ would be the best estimate of the outputs. This set of values is used as the basepoint to calculate the new parameter estimates from Eq. (3.37).

The operation can be linearized to solve for the relationships between $(\hat{x}, \hat{\theta}, \hat{\phi})$ near (x, θ, ϕ) as follows:

$$\delta\hat{x} = \hat{x} - x \qquad (3.41a)$$

$$\delta\hat{\theta} = \hat{\theta} - \theta \qquad (3.41b)$$

$$\delta\hat{\phi} = \hat{\phi} - \phi \qquad (3.41c)$$

The following expression results from expanding Eq. (3.38):

$$\delta \hat{x} = C^{-1}[g_\theta(\hat{x},u)\delta\hat{\theta} - g_w(\hat{x},u)w] \qquad (3.42a)$$

$$C = [I - g_{o_X}(\hat{x},u) - g_{\theta_X}(\hat{x},u)\hat{\theta}] \qquad (3.42b)$$

In this form, the difference term on the left hand side of Eq. (3.42) is correlated with the terms used to calculate the right-hand side through errors in inputs, u. Defining

$$\delta\hat{y}(i) = \hat{y}(i) - y(i) \qquad (3.43)$$

Eq. (3.42) can be rewritten in a more convenient form as follows:

$$\delta\hat{y} = BC^{-1}[g_\theta(\hat{x},u)\delta\theta - g_w(\hat{x},u)w + h_\phi(\hat{x},u)\delta\hat{\phi} + v] \qquad (3.44a)$$

$$B = I + h_{\phi_X}(\hat{x},u)\hat{\phi} \qquad (3.44b)$$

or, for N measurements indexed on i,

$$\Delta y_i = H_i \delta\overline{\theta} + \Gamma_i \overline{v} \qquad i=1,\ldots,N \qquad (3.45a)$$

where

$$\Delta y_i = \hat{y}(i) - y(i) \qquad (3.45b)$$

$$\overline{\delta\theta}^T = [\delta\hat{\theta}^T \mathrel{\vdots} \delta\hat{\phi}^T] \qquad (3.45c)$$

$$\overline{v} = [v^T \mathrel{\vdots} w^T] \qquad (3.45d)$$

$$H_i = [B_i C_i^{-1} g_\theta(\hat{x}_i,u_i) \mathrel{\vdots} h_\phi(\hat{x}_i,u_i)] \qquad (3.45e)$$

$$\Gamma_i = [I \mathrel{\vdots} -B_i C_i^{-1} g_w] \qquad (3.45f)$$

34

The N measurements in Eq. (3.45) can be used to update the parameter estimates using the sequential least squares procedure as follows:

$$\overline{\delta\theta}(n+1) = \overline{\delta\theta}(n) + M_{n+1}H_n\overline{R}_n^{-1}[\Delta y_n - H_n\overline{\delta\theta}(n)] \qquad (3.46)$$

$$n=1,\ldots N$$

$$M_{n+1}^{-1} = M_n^{-1} + H_n^T\overline{R}_n^{-1}H_n \qquad (3.47)$$

where

$$\overline{R}_n = \Gamma_n \, cov(\overline{v}) \, \Gamma_n^T$$

and M_o measures the uncertainty in the parameter values at the beginning of the process.

The procedure assumes that the measurement errors and error statistics are known and that the parameters are constant. In an engine environment, these assumptions may not be satisfied causing inaccurate parameter estimates. Also, the parameter estimates may be significantly biased because of correlations between the dependent and independent variables in Eq. (3.45).

The sequential algorithm presented in Eqs. (3.46) and (3.47) is appropriate for situations in which data is continuously received and not available after processing. This scenario is typical of on-line, real time processing systems. The off-line performance data processing scenario is different. Groups of data points (5-10 measurements) are received for an engine. This data is available for processing as long as necessary. It is discarded after processing. Figure 3.2 illustrates the information flow.

An algorithm for using data in this format is presented below [46]. The likelihood function for estimating the engine state and degradation parameters for N measurements is
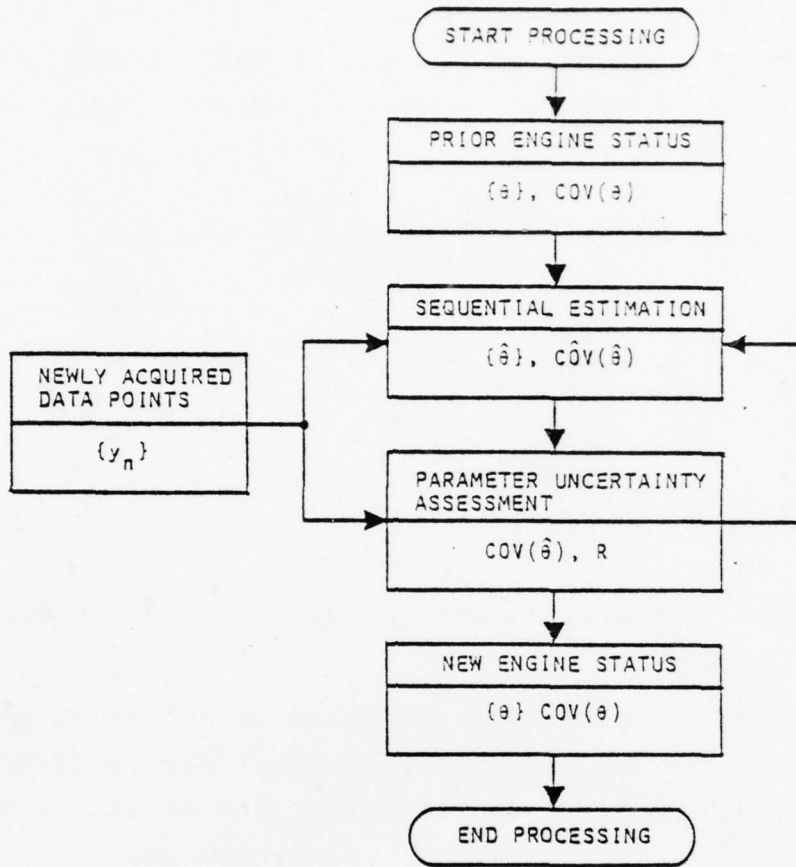
Figure 3.2   Parameter Estimation Process

$$J(x(n),n=1,N;\theta) = \sum_{n=1}^{N} \gamma_n^T R_n^{-1} \gamma_n + \overline{\theta}^T M^{-1} \overline{\theta} \tag{3.48}$$

$$\gamma_n = y_n - \hat{y}_n \tag{3.49}$$

$$\hat{y}_n = g_o(\hat{x}_n, u_n) + g_\theta(\hat{x}_n, u_n)\hat{\theta} + h_\phi(\hat{x}_n, u_n)\hat{\phi} \tag{3.50}$$

where M is an initial parameter covariance estimate.

The functional, J, is iteratively minimized. An initial estimate of the parameters, $\hat{\theta}, \hat{\phi}$ from previous runs is assumed for the N data points. These values are used to estimate the engine states, $\hat{x}_n$, at each point from Eq. (3.42). Then,

36

Eq. (3.46) is used to estimate the updated parameter estimates, $\hat{\theta}$, $\hat{\phi}$, from the state estimates. This procedure is iteratively executed until the estimates $\hat{x}$, $\hat{\theta}$, $\hat{\phi}$ converge to a constant value.

After a group of data has been used to estimate $\hat{\theta}$, $\hat{\phi}$, $\hat{x}$, the residuals can be used to update the noise estimates and the estimate uncertainty. The sensor noise covariance is estimated from the residuals,

$$\hat{R} = \text{cov}_N(\Delta\hat{y}) \tag{3.51}$$

where $\text{cov}_N(\cdot)$ is the N sample covariance of the final residuals of the estimator. Using $\hat{R}$, the uncertainty in the parameter estimates for the current record can be written:

$$\text{cov}(\overline{\theta}) = \left[\sum_{n=1}^{N} H_n R H_n \right]^{-1} \tag{3.52}$$

This can be combined with the original covariance estimates using an exponentially fading memory filter,

$$M_{N+1}^{-1} = M_0^{-1} + \rho[\text{cov}(\overline{\theta}) - M_0^{-1}] \tag{3.53}$$

The value of ρ is chosen so that the filter "ignores" measurements taken at N_f time points prior to N where N_f is given approximately as follows:

$$N_f = 3/\ln(\rho) \quad . \tag{3.54}$$

This algorithm will provide estimates of the parameters for data taken in an essentially finite window covering a portion of the engine operating period. The system can also be reinitialized after engine maintenance or trim.

An algorithm is briefly described above which uses parameter estimation to establish values of engine parameters from static data. In section 3.3.1, a procedure for developing the models used in this algorithm is described. In Section IV, considerations important in applying this algorithm to the F100 gas path are presented.

3.3.2 Model Development Techniques

The parameter estimation algorithm described in Section 3.3 uses a mathematical model of engine performance and derivatives which is developed from a detailed simulation of the engine. The calculation of the best form of the model is described below. Parameter estimation results are closely tied to the model used. A method of model selection is presented which allows a system approach to formulating fault parameters which can be accurately identified and which reflect the actual status of the engine.

3.3.2.1 Development of the Baseline Model

The engine baseline model describes the set of measured variables as a function of other variables and a set of more accurately measured independent quantities. This relationship is written as follows:

$$x = g_o(x,u) \tag{3.55}$$

A data base of generic engine operating points is formed. For the aircraft turbine, this requires generation of typical operating data at various points in the flight envelope where measurements are to be taken. Data should be generated in approximate proportion to the density of measurements which will be processed during actual-flight operation. The windows of data acquisition can be written as follows (as an example):

38

$$T_{2min} < T_2 < T_{2max}$$

$$P_{2min} < P_2 < P_{2max}$$

$$0 < M < M_{max} \qquad\qquad (3.56)$$

$$(W_f/\sqrt{\theta}\delta)_{min} < W_f/\sqrt{\theta}\delta < (W_f/\sqrt{\theta}\delta)_{max}$$

$$\gamma_{imin} < \gamma_i < \gamma_{imax} \quad \text{(geometry positions)}$$

The pressure, temperature and Mach number constraints bound the flight envelope. The fuel flow and geometry settings will be independently specified and chosen from typical values. The values of inputs are set independently of control schedules, feedback, etc. The number of points in a particular region should correspond to the expected data frequency. The models are developed using a least squares regression analysis to determine the model for each x_j:

$$J^* = \min_{\beta} [x_j - g_o(x_j^*, u)]^2 \qquad\qquad (3.57)$$

where the baseline function, $g_o(x_j^*, u)$ has the form:

$$g_o(x_j^*, u) = \sum_{i=1}^{q} \beta_i t_i(x_j^*, u) \qquad\qquad (3.58)$$

and the regression coefficients, β_i, are chosen so that the terms in the equation, $t_i(x_j^*, u)$, match the data. The variables in the model do not contain the dependent variable, x_j. The vector of independent variables for the j-th equation can be written as follows:

$$x_j^* = \begin{bmatrix} x_1 \\ \vdots \\ x_{j-1} \\ 0 \\ x_{j+1} \\ \vdots \\ x_n \end{bmatrix} \qquad\qquad (3.63)$$

The terms, $t_j(x_j^*,u)$, consist of polynomials in dependent and independent variables. The independent variables, u, are chosen as a set of accurately measured quantities which determine the engine state uniquely. The choice of these variables may be altered and the effect on the model accuracy determined.

The regression in Eq. (3.57) is performed on many possible combinations of model terms $t_j(x_j^*,u)$ and the best regressions at various levels of parameterization are determined.

The regressions are designed to parameterize the dependent variables with the minimum error and the minimum number of terms. The number of regression terms is reduced because the equations are allowed to contain variables which are independent in other equations. This procedure can lead to poorly invertible models. The selection of appropriate model terms must be accomplished using the criterion of equation accuracy and over-all invertibility.

Consider the vector model,

$$x = g_o(x,u) + \varepsilon \tag{3.60}$$

where ε is the fit error for each regression. A group of operating points is selected and the model is inverted in these regions as follows.

Given (x_{io}, u_{io}) is an equilibrium point, then

$$\delta x_i + x_{io} = g_o(x_{io}, u_{io}) + g_{ox}(x_{io}, u_{io})\delta x$$
$$+ g_{ou}(x_{io}, u_{io})\delta u \tag{3.61}$$

or

$$\delta x = [I - g_{ox}(x_{io}, u_{io})]^{-1} g_{ou}(x_{io}, u_{io})\delta u \tag{3.62}$$

The <u>overall</u> modeling error due to fit errors and in knowledge of u can be evaluated using the following criterion function (p is the number of measurements and r is the number of test flight conditions):

$$J_{FIT} = \frac{1}{p} \sum_{i=1}^{p} [\sigma_{\varepsilon_i}^2] + \frac{1}{r} \sum_{i=1}^{r} \text{tr}[(I-g_{ox})^{-1}g_{ou}Qg_{ou}^T(I-g_{ox}^T)^{-1}]$$

$$\tag{3.63}$$

where Q is the expected covariance of the errors in the independent variable, u, or

$$Q = \text{diag}[\sigma_{u_1}^2, \sigma_{u_2}^2, \ldots, \sigma_{u_m}^2] \tag{3.64}$$

The performance index, J_{FIT} can be evaluated for several parameterizations of the model and the most accurate expression chosen.

41

3.3.2.2 Development of Performance Parameters

After an accurate model is developed for the generic base-
lines, the data base must be increased to include data representing
the deteriorated engine. These effects will include efficiency
changes, area changes, pressure drops, flow changes as well as
disturbances due to bleed effects and control actuator hyste-
resis.

There are a large number of points represented by complete
combinations of these effects. The linear characteristics of
the model can be used to reduce the computation overhead.
Values of fault parameters can be varied, one at a time, at a
selected group of operating points which span the envelope.
The computer resources for this type of data base are not over-
whelming.

The model for the fault parameters, instrumentation effects
and random errors is written below

$$\Delta y = H_\theta \theta + H_\phi \phi + \Gamma \overline{v} \tag{3.65}$$

where the matrices H_θ, H_ϕ, and Γ are functions of the
flight condition and are defined in Section 3.3. The covari-
ance of the estimation error for the maximum likelihood (mini-
mum variance) estimate must satisfy the following relationship

$$M = \partial^2 J / \partial \overline{\theta}^2 \tag{3.66a}$$

where J is the log likelihood function of the estimation
problem. It can be shown that the following inequality is
valid [47]:

$$\text{cov} \begin{pmatrix} \theta \\ -- \\ \phi \end{pmatrix} \geq \begin{pmatrix} M_{\theta\theta} & \vdots & M_{\theta\phi} \\ ---- & \vdots & ---- \\ M_{\phi\theta} & \vdots & M_{\phi\phi} \end{pmatrix}^{-1} \triangleq M^{-1} \tag{3.66b}$$

42

where $(\theta^T \vdots \phi^T)^T$ is assumed to include all possible variable engine and instrumentation parameters. The matrix M is calculated as follows:

$$M = \frac{1}{N} \sum_{i=1}^{N} (H_\theta \vdots H_\phi)(\Gamma R \Gamma^T)^{-1} \begin{bmatrix} H_\theta^T \\ --- \\ H_\phi^T \end{bmatrix} \mu_i \qquad (3.67a)$$

$$\sum_{i=1}^{N} \mu_i = 1 \qquad (3.67b)$$

where the sum is taken over N flight points at which data is taken with fractional frequency μ_i. In the algorithm development, a representative group of flight points and frequencies is chosen. This relation may be expanded as follows:

$$M = \mu_1 M_1 + \mu_2 M_2 + \ldots + \mu_N M_N \qquad (3.68)$$

In general, if p measurements are taken at each point, only p or less parameters can be estimated. However, since the sensitivities vary with flight condition, it is possible to estimate far more parameters than the number of measurement variables using this procedure. The precise number and their accuracy is calculated using the following technique, developed in Ref. 1.

Consider the parameter vector $(\theta^T \vdots \phi^T)$ and reorder this vector into elements $(\theta_r^T \vdots \theta_e^T)^T$ where θ_r parameters will be estimated and θ_e parameters will be ignored.

The covariance of the estimates of θ_r using the full set of equations from Eq. (3.66) is

$$\text{cov}(\theta_r) = M_{rr}^{-1} + M_{rr}^{-1} M_{re} (M_{ee} - M_{er} M_{rr}^{-1} M_{re})^{-1} M_{er} M_{rr}^{-1} \qquad (3.69)$$

43

where

$$M = \begin{pmatrix} M_{rr} & \vdots & M_{re} \\ ---- & \vdots & ---- \\ M_{er} & \vdots & M_{ee} \end{pmatrix} \qquad (3.70)$$

Since the estimates are unbiased

$$cov(\theta_r) = MSE(\theta_r)$$

where $MSE(\cdot)$ is the mean square error. In the case when
fewer parameters are actually estimated, i.e., θ_e parameters are
ignored, it can be shown that the estimates are biased and the
mean square error is as follows:

$$MSE(\theta_r) = M_{rr}^{-1} + M_{rr}^{-1} M_{re} D(\theta_e) M_{er} M_{rr}^{-1} \qquad (3.71)$$

where $D(\theta_e)$ is the approximate uncertainty level in the ex-
traneous parameters,

$$D(\theta_e) = diag(\Delta\theta_e^2) \qquad (3.72)$$

Comparing Eqs. (3.70) and (3.71), the accuracy of the estimate
of θ_r improves if θ_e parameters are not estimated and

$$D(\theta_e) < (M_{ee} - M_{er} M_{rr}^{-1} M_{re})^{-1} \qquad (3.73)$$

i.e., $D(\theta_e) - (M_{ee} - M_{er} M_{rr}^{-1} M_{re})^{-1}$ is positive definite.

In order to evaluate the accuracy of an estimator for all
subsets of the parameters using Eq. (3.71), all possible
combinations of the parameter sets must be evaluated. This is
an extremely tedious procedure if Eq. (3.71) is used directly.
However, there is an algorithm available to efficiently and
economically evaluate the optimal subset of estimated parameters.
This procedure is based on complete enumeration of all possible
subset combinations in a systematic order. The covariance

estimates are available for each subset from the preceding subset using a simple calculation on a portion of the information matrix. A detailed description of this technique and examples of its application to the modeling problem are included in the next interim report for this effort.

An alternative procedure aids in qualitative analysis for the important parameter effects. The information matrix for the full system, e.g., Eq. (3.69), is diagonalized and the eigenvalue spectrum is examined. Large eigenvalues indicate that the linear combinations of parameters determined by the corresponding eigenvectors are accurately identified with flight data. Small eigenvalues imply that the estimated covariance of the linear combination of parameters corresponding to that modal direction is large. The information matrix can be partitioned into groups of certain parameters by associating the large eigenvalues with these parameters. Equation (3.71) can be used to calculate the estimation accuracy for the reduced parameter vector using an estimate of the magnitude of the ignored parameters.

This procedure allows flexibility in the choice of retained parameters and a quantitative measure of parameter identifiability and accuracy tradeoffs. The resulting set of estimated variables along with the associated generic baseline and sensitivity system can be directly incorporated into the sequential estimation algorithms discussed in Section 3.3.

3.4 TREND ANALYSIS

In the static analysis described in Section 3.3, the parameter values were assumed constant over the data. Provision for a "fading memory" construction was discussed in the development of the algorithm. In this section, the augmentation of the static model identification equations with simple trend models will be discussed as well as the association of an appropriate time variable with the trends.

45

3.4.1 Trending Equations

The trending process assumes a linear relationship exists between a function mapping the data acquisition times to changes in the parameter values. The simplest mapping is the association of the sampled point with the time of the sample. This time point may be calendar time, flight time, engine operating hours, or some other function of the usage period of the turbine. This functional mapping, for example, specifies the separation of the data points on a sequential plot. In this section the time of the kth sample, t_k, will be associated with the kth variable. In the next section, some properties of a function, $f(t_k)$, will be discussed and techniques for developing appropriate forms from flight data will be described.

The data may be written in the ordered sequence given below:

$$\{y_k, \ u_k, \ t_k\} \qquad k = 1,N \qquad t_{k-1} \le t_k$$

A _dynamic_ representation of parameter variations may be formulated as linear motion, or

$$\delta\theta(k+1) = \delta\theta(k) + r(k)[t_k - t_{k-1}] \qquad (3.74)$$

$$r(k+1) = r(k) + w_r(k) \qquad (3.75)$$

$$\Delta y = H_\theta \delta\theta + H_\phi \delta\phi + v \qquad (3.76)$$

where $r(k)$ is assumed to be a constant or slowly varying deterioration rate and w_r is a nominal noise sample which reflects the uncertainty in this variable.

Two approaches may be used to estimate $\theta(k)$ and $r(k)$. Equations (3.74)-(3.76) can be used as the basis of a Kalman filter for the state $(\delta\theta \mid r)$ and an algorithm can be designed

46

to estimate these quantities. The dynamics of the system are
written as follows:

$$\begin{bmatrix} \delta\theta(k+1) \\ r(k+1) \\ \delta\phi(k+1) \end{bmatrix} = \begin{bmatrix} 1 & \Delta t & 0 \\ 0 & 1 & 0 \\ 0 & 0 & 1 \end{bmatrix} \begin{bmatrix} \delta\theta(k) \\ r(k) \\ \delta\phi(k) \end{bmatrix} + \begin{bmatrix} 0 \\ 1 \\ 0 \end{bmatrix} w_r(k) \qquad (3.77a)$$

where

$$\Delta t = t_{k+1} - t_k \qquad (3.77b)$$

This may be written as follows:

$$z(k+1) = \phi_k z(k) + \Gamma w(k) \qquad (3.78)$$

$$\Delta y(k) = H_k z(k) + v(k)$$

where

$$z(k)^T = [\delta\theta(k)^T \;\vdots\; r(k)^T \;\vdots\; \delta\phi(k)^T] \qquad (3.79)$$

The estimate of $z(k)$ is $\hat{z}(k)$ given as follows:

$$\hat{z}(k+1) = \bar{z}(k) \qquad (3.80)$$

$$\bar{z}(k) = \hat{z}(k) + K_k[\Delta y(k) - H_k\hat{z}(k)] \qquad (3.81)$$

$$K_k = P_k H_k^T R^{-1} \qquad (3.82)$$

$$P_{k+1} = P_k\phi_k + \phi_k^T P_k + \phi_k H_k P_K\phi^T (R+HP_kH^T)^{-1}\phi_k^T H_k^T P_k\phi + Q \qquad (3.83)$$

In these equations, the matrix, P_k, represents the
uncertainty in the parameter estimates after processing data up
to $t = t_k$. The initial condition, P_o, represents the a priori

47

uncertainty on the parameter values, i.e., before any measurements are taken. The disturbance process, w_k, is assumed to be known, white, zero mean with constant covariance, Q. In practice, this can be estimated from the amount of variability in the rate or from the performance of the filter after a group of data have been processed [49].

A steady state representation of the gain Eqs. (3.82) and (3.83) can be more efficiently used. There are problems in filter convergence for this model due to the lack of "disturbability" of some of the bias states, $\delta\phi$. The most straightforward method to avoid this problem is to use pole placement for these neutrally stable modes to assure convergence of the filter.

An alternate formulation is the static, extended Kalman filter algorithm for both the parameters and the state [46]. This algorithm is presented for completeness below. The state model is given as follows:

$$x(k+1) = x(k) + w_x(k)$$

$$\delta\theta(k+1) = \delta\theta(k) + r(k)(t_{k+1} - t_k) + w_\theta(k) \qquad (3.84)$$

$$r(k+1) = r(k) + w_r(k) \ .$$

The measurements are defined by the equation:

$$y = g_o(x,u) + g_\theta(x,u)\delta\theta + g_\phi(x,u)\delta\phi + v \qquad (3.85)$$

In this case, $w_x(k)$ is assumed $N(0,Q_x)$ where Q_x is chosen large enough to ensure the engine state at the (k+1)st point is not correlated (to a practical degree) with the state at k, as would be the case in sparsely sampled data. The covariance of w_θ, $N(0,Q_\theta)$ represents a priori information on the parameters. The uncertainty in the rate is w_r, $N(0,Q_r)$ and in the measurement is v, $N(0,R)$ and

48

$$\hat{z}(k)^T = [\hat{x}(k)^T \mid \delta\hat{\theta}(k)^T \mid \hat{r}(K)^T \mid \delta\hat{\phi}(k)^T] \qquad (3.86)$$

is given from the following recursion,

$$\hat{z}(k+1) = \hat{z}(k) + P_k H_k^T R^{-1} [\Delta y(k) - H_k z(k)] \qquad (3.87)$$

where

$$\Delta y(k) = H_k z(k) \qquad (3.88)$$

and

$$H_k = \left[\frac{\partial g_o}{\partial x} \mid g_\theta \mid 0 \mid g_\phi \right] \Bigg|_{\substack{x = \hat{x} \\ \delta\theta = \delta\hat{\theta} \\ \delta\phi = \delta\hat{\phi}}} \qquad (3.89)$$

The optimal gain can be calculated for the data and the algorithm can be applied in the manner described in Ref. 46.

Alternate methods of parameter estimation can also be used to trend the parameter data. The maximum likelihood method is perhaps the most accurate. This procedure requires a list of the data points and iteratively processes the entire data record to achieve its estimate. Accurate estimates of the small deterioration rates within the noise level of the measurements will probably require this type of processing. For a more complete discussion of these procedures, see Ref. 47.

3.4.2 Time Variable Correlations

The trending procedures for aircraft turbines can be formulated as standard parameter estimation problems as discussed in Section 3.4.1. An important aspect is the definition of a time variable to model deterioration as a constant rate, $r(k)$. Assuming that deterioration is continuous, i.e., step changes due to foreign object damage, structural failure, maintenance action,

49

etc., do not occur, it would be expected that a <u>constant</u>
deterioration rate,

$$r = \frac{\partial \theta}{\partial t^*} \tag{3.90}$$

exists for a function $t^*(t)$.

The time variable t^* should be influenced by the phen-
omenological processes within the engine that cause deteriora-
tion. Maintenance procedures, e.g., turbine module replacement,
should influence the performance parameter levels, $\delta\theta$, but
not the deterioration rates. Thus, the trending procedure has
the potential to be extremely useful in maintenance assessment
and prognostication if the appropriate correlation function,
t^*, can be identified.

Previous trending systems have used many choices for
the variable t^*. Early monitoring schemes trended the engine
variables versus engine time. In turbine engines, the power
level, temperature and hence stress levels vary significantly
from flight to flight. An approach to developing this correla-
tion is embodied in the advanced mission test (AMT) [22] concept
currently being employed during development of military air-
craft powerplants. It is assumed that deterioration occurs
mainly during power modulation. Characteristic power transients
are formulated for each aircraft mission profile. Engines are
then tested with these transients and equivalent engine hours
are tabulated. Periodically performance tests and rebuilds as-
sess the levels of deterioration and performance shifts which
have occurred. This procedure can be related to the development
of the time-like variable, t^*, which, in the case of the AMT,
is experimentally related to engine hours using a standard mis-
sion profile and the assumption that deterioration rates in
steady state are negligible.

There are several approaches to the determination of the trending variable. An example of the concept is presented to illustrate the problem. Figure 3.3 shows plots of measured and derived data. The measurements are taken at many flight points and power conditions. The parameter estimates should have only
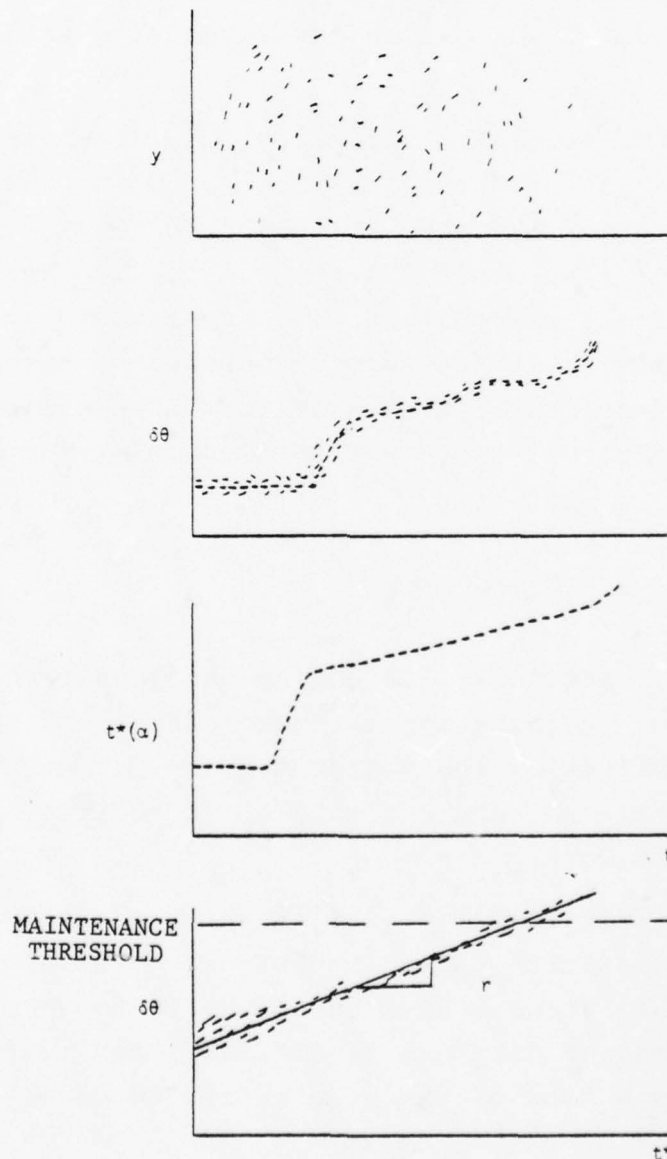

Figure 3.3 Utilization of a Time Like Variable, t*, to Measure Rates of Engine Deterioration

51

low frequency components associated with the deterioration process. The function t^* $(t, \alpha_1, \alpha_2, \ldots, \alpha_3)$ is sought which will map t to t^* given values of intermediate variables $\alpha_1 \ldots \alpha_3$. Parameter estimates plotted against t^* form a nearly straight line. This functional form can be used for all engines to assess: (a) the status of the engine, (b) the value of t^* when a maintenance limit is reached, (c) the time (in engine hours) until the deterioration limit is reached given nominal values of $\alpha_1, \ldots, \alpha_r$ which are associated with the mission.

The performance associated variables, α, represent measurements in the gas path that are monitored in real time or sampled in the data. Examples of these variables might be: (a) engine time, (b) time above 85% power, (c) time above a specified turbine inlet temperature, (d) temperature profile (spread) characteristics at the turbine inlet, (e) number of accelerations and decelerations greater than a specified magnitude, and (f) integrals of speed and turbine inlet temperature which are measured in real time.

3.5 MONITORING TRANSIENT PARAMETERS

In the previous sections, the engine has been treated as a quasi-static system. Degradation has been determined by changes in operating line values of the measurements. One drawback of this approach is that one cannot always differentiate between engine and sensor failures.

To achieve failure isolation, utilization of transient data from continuous or discrete control inputs is attractive. Initial attempts at this process have been made in Europe [34,36]. The utility of transient data can be qualitatively justified by examining the expansion of the general system model as follows:

52

$$\dot{x} = f(x_o, u_o, \theta_o) + f_x \delta x + f_u \delta u + f_\theta \delta \theta$$

$$+ \frac{1}{2} (f_{\theta\theta} \delta \theta^2 + f_{xx} \delta x^2 + f_{uu} \delta u^2 + 2 f_{xu} \delta u \delta x$$

$$+ 2 f_{x\theta} \delta x \delta \theta + 2 f_{u\theta} \delta u \delta \theta) \qquad (3.91)$$

where

$$f_x = \partial f / \partial x \Big|_{\substack{x = x_o \\ u = u_o}} , \text{ etc.} \qquad (3.92)$$

Assuming that an equilibrium point is chosen for the expansion, Eq. (3.91) can be rewritten as follows:

$$\dot{x} = (f_x + f_{x\theta} \delta \theta) \delta x + (f_u + f_{u\theta} \delta \theta) \delta u + (f_\theta + \frac{1}{2} f_{\theta\theta} \delta \theta) \delta \theta$$

$$+ \frac{1}{2} f_{xx} \delta x^2 + \frac{1}{2} f_{uu} \delta u^2 + f_{xu} \delta u \delta x \qquad (3.93)$$

In the static problem, the choice of linearization point forced

$$\delta \dot{x} = 0$$

and $\qquad\qquad\qquad\qquad\qquad\qquad\qquad\qquad\qquad$ (3.94)

$$\delta u = 0 \quad .$$

The remaining terms represented the steady offset in δx due to $\delta \theta$. In the transient case, δx, δu are assumed time varying. The time varying response is not greatly influenced by instrument biases and other steady state effects. For this case, the equations reduce to the following:

$$\dot{x} = (f_x + f_{\theta x} \delta \theta) \delta x + (f_u + f_{u\theta} \delta \theta) \delta u + \theta(\delta^2) \qquad (3.95)$$

If the higher order terms in Eq. (3.95) are neglected except for the dependence of the transient terms on the fault parameters, the linear system resulting is as follows:

$$\dot{x} = F(\theta)\delta x + G(\theta)\delta u \tag{3.96}$$

Terms of the form $f_{x\theta}\delta\theta$ may be comparable to the terms f_x for small values of $\delta\theta$. If this is the case and these parameters can be estimated from the measurements, then an alternate class of fault coefficients may be derived.

As an initial experiment, two linear models were generated for the F100 turbofan engine at idle power. One model used nominal values of the engine build parameters. The other used values which represented a fully deteriorated engine. Linearized dynamical parameters are compared in Table 3.1. These results indicate that the second order fault parameters may be significant in these transient equations. Engines in many practical situations (e.g. military missions) operate with a continuous series of small throttle motions. This type of input environment is suited for real-time parameter estimation. Data can be acquired nearly continuously in flight and storage or recording

Table 3.1

Effect of Deterioration, Power Extraction, and
Bleed on System Equations
(Sea Level Static/Idle)

TIME CONSTANTS	NOMINAL	INSTALLATION EFFECTS	UNITS
Fan Stream	$\omega_n = 5.6, \zeta = .91$	$\omega_n = 5.1, \zeta = .92$	sec^{-1}
Core Stream	$1/\tau = +0.75$	$1/\tau = 0.72$	sec^{-1}

DYNAMIC ELEMENTS	NOMINAL	INSTALLATION EFFECTS	UNITS
$\delta\dot{N}_1/\delta N_1$	+0.58	-0.84	sec^{-1}
$\delta\dot{N}_2/\delta N_2$	-5.04	-4.40	sec^{-1}
$\delta\dot{P}_6/\delta P_6$	-0.23	-2.45	sec^{-1}
$\delta\dot{N}_1/\delta P_6$	-6250	-3620	(RPM/PSIA) sec^{-1}
$\delta\dot{P}_6/\delta N_1$	-0.0017	-0.00041	(PSIA/RPM) sec^{-1}

is not required. At the end of the mission, the updated fault coefficient can be retrieved and parameter trending procedures performed against previous engine operation.

Maximum likelihood parameter estimation procedures for sequential processing are reviewed in detail in Refs. 1 and 47. A significant fallout of this on-line algorithm is an accurate failure detection method for system parameter jumps. These sharp parameter changes can be caused by sensor failure, foreign object damage, structural failure of gas path components, fuel leaks, manifold clogs, or control malfunctions of certain types. The application of this procedure is illustrated in Figure 3.4 for a simple model of a turbojet driven by small deterministic inputs and random disturbances.

The simple turbojet speed model can be written as follows:

$$\frac{dN}{dt} = \frac{-1}{\tau} (N - u - w) \tag{3.97}$$

where u is modeled as small commanded speed inputs of random width and w is a white, Gaussian disturbance process, $N(0,Q)$. The rotor speed is measured and the engine time constant, τ, is estimated. At time $t = t_J$, τ abruptly changes value from 1 sec to 2 sec. The estimate of the parameter τ and the predicted disturbance covariance are shown. The system equations for this example are as follows:

Estimator: $$\dot{\hat{x}} = (1/\hat{\tau})(\hat{x} - u) + \hat{k}(y - \hat{x}) \tag{3.98}$$

Observation: $$y_k = x_k + v_k$$

$$J^* = \min_{\hat{t}, \hat{k}} \sum_{i=1}^{N} (y_k - \hat{x}_k)^2 \tag{3.99}$$
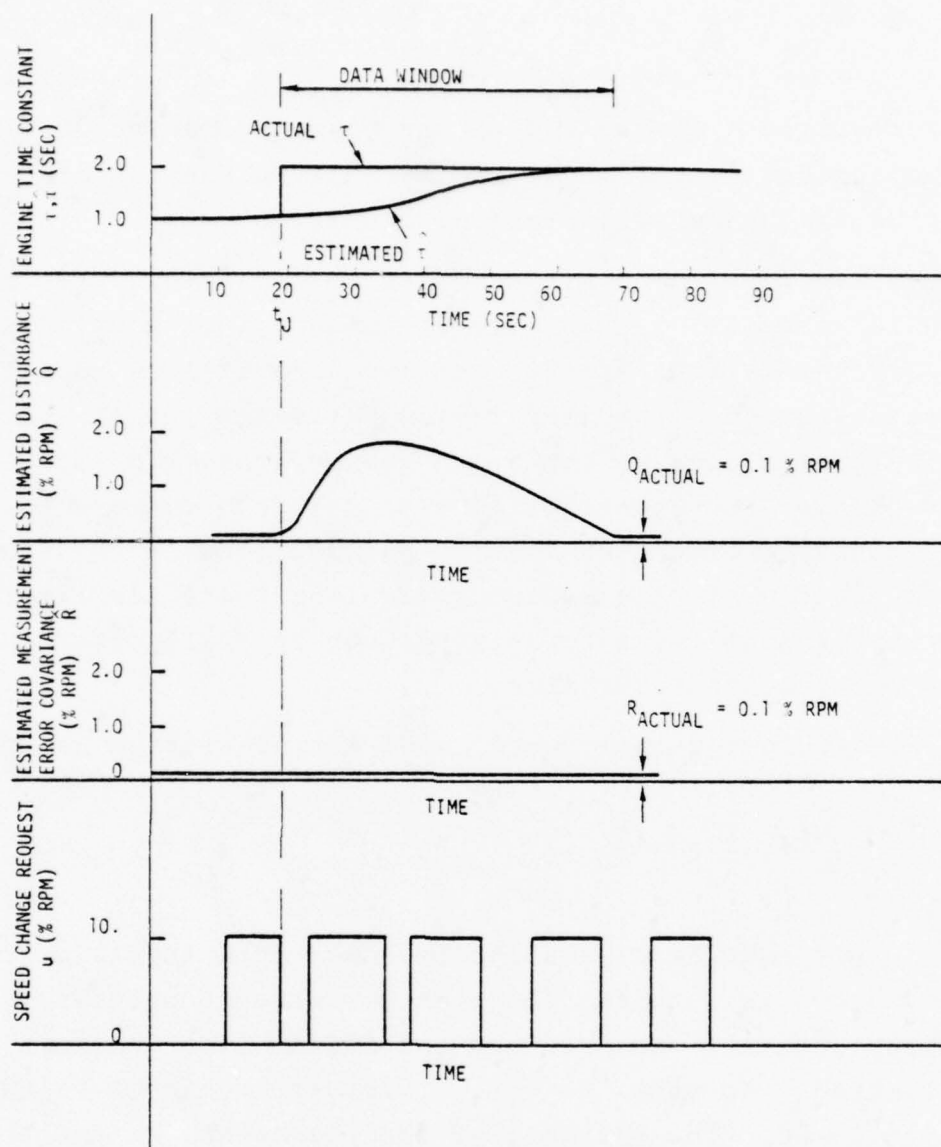
Figure 3.4   Example of Parameter Estimation with a Jump in an
Engine Parameter Showing Large Increase in Disturbance
Covariance During Data Window Containing Jump

The results indicate that for the finite data length, the jump
in the parameter value causes a significant increase in the esti-
mated disturbance level.   This occurs because behavior not
modeled by the linear dynamics is attributed to the disturbance
process.   Failure detection techniques can utilize this sharp

rise in estimated Q to quickly and accurately determine sharp
plant variations. It should be noted that no a priori knowledge
of the expected value of the time constant is required to imple-
ment the suggested procedure. The monitoring of the shift in the
parameter estimate would produce a far less robust detection
technique. In this case, the 2:1 change in the time constant
yields a 20:1 change in the estimated disturbance. The approach
also functions in the presence of actual disturbances, inputs,
and measurement errors including biases.

3.6 SUMMARY

This chapter has developed a unified framework within which
the requirements of performance monitoring, trending, and transi-
ent fault detection/isolation may be achieved. This framework
is based on maximum likelihood methods for state and parameter
estimation. Formulating the problem from the more general view-
point, algorithms for the particular engine monitoring objectives
are synthesized.

SECTION IV

PERFORMANCE MONITORING FOR THE F100 TURBOFAN ENGINE

4.1 INTRODUCTION

The feasibility of the performance monitoring approach is investigated for the F100 turbofan engine. The objective of this study is to utilize a detailed nonlinear digital simulation of the F100 engine to create a preliminary engine data base. Models of the generic data are created and the predicted accuracies calculated. A more detailed set of models and a more extensive set of engine data will be utilized for full system development at a later date.

In this section, the F100 Engine Diagnostic System (EDS) data acquisition is discussed. Simulation programs are utilized in the development of an initial set of quasi-linear regression models for the envelope of data acquisition. These models are discussed and proposed modifications to the generation procedure are presented to improve the overall accuracy. Finally, in-flight acquisition algorithms are reviewed with the aim of improving data quality.

4.2 F100 ENGINE DIAGNOSTIC SYSTEM

The F100 engine diagnostic system (EDS) program is an on-going development effort sponsored by the Air Force involving the engine and airframe manufacturer of the F-15/F-16 flight systems. The EDS program is chartered to develop and flight test practical avionics hardware and software to acquire and process logistically meaningful fault and deterioration data for the engine.

The EDS system uses a series of engine transducers mounted
in conveniently located positions in the gas path. Engine, as
well as lubrication and fuel distribution systems, are monitored
to detect out-of-limit behavior. Subsystem variables are sampled
continuously by an engine-mounted, fuel-cooled microprocessor
system, the engine multiplex (EMUX). This processor is connected
via a data bus to an airframe-mounted avionics computer dedicated
to the EDS, the data processing unit (DPU). The DPU stores data
consisting of time histories of key engine variables before,
during, and after an event is detected. This data is later
recoverable for general analysis to isolate faulty behavior.

In addition to fault information, steady state data is
acquired in flight for performance and trend checks. These
data "points" are recorded when aircraft and throttle states
have not changed significantly for a predetermined settling
period. The limits of altitude and throttle are shown in
Table 4.1. Analysis by the engine manufacturer has indicated
that these preliminary settling times are necessary to achieve
engine operation with the slower heat sink and temperature lag
processes sufficiently equilibriated for accurate steady state
measurement.

Data acquired by the DPU for performance and trend consists
of several samples which are processed to remove noise and are
stored in the DPU. After a flight, the data generated in flight
is passed to one of two portable units, the data collection unit
(DCU) or the data display unit (DDU) for remote processing.
The DDU is used for engine troubleshooting and trim. It is
connected when trouble flags appear in the DPU panel. The DCU
is used under normal conditions to retrieve stored data for
trending and analysis. This data is made available for on-sight
processing or off-base macroprocessing via telephone MODEM link.

The EDS provides state-of-the-art avionics engine diagnostic
capability to the F-15/F-16 fleet. Automated troubleshooting

60

Table 4.1

Data Collection Windows for
EDS Flight Test Program

TYPE	WINDOW CONDITIONS
IN-FLIGHT PERFORMANCE CHECK	PLA $\geq$ 83° FOR 140 SEC 83° $\leq$ PLA $\leq$ 39° FOR 10 SEC 3000 $\leq$ H $\leq$ 25,000 FT. ANTI-ICE OFF
TREND DATA COLLECTION CONDITIONS	40° $\leq$ PLA $\leq$ 89° PLA = CONSTANT $\pm$10° FOR 175 SEC. PLA - CONSTANT $\pm$1° FOR LAST 5 SEC. N1 = CONSTANT $\pm$60 RPM FOR ⁻ SEC. N2 = CONSTANT $\pm$60 RPM FOR ⌐C. Pb = CONSTANT $\pm$0.5% OF POINT FOR 5 SEC. 0 $\leq$ MO $\leq$ .7 0 $\leq$ ALT $\leq$ 10K FT ANTI-ICE OFF

and trim procedures can be performed utilizing the sophisticated
DDU minicomputer. In addition, the on-board data acquisition
capability provides an excellent source of well-controlled in-
flight engine data. This information can be directly processed
by performance analysis and trending algorithms to accurately
determine engine status and identify engine deterioration pro-
cesses.

The engine transducers which will be used for EDS perform-
ance and trend measurements are listed in Table 4.2. These
transducers can be installed without major modification to the
existing engine structure. In most cases these sensors will
replace existing F100 sensors providing improved accuracy.
Sensors are provided with electronic interfaces. Critical
instrument accuracy specifications involve long-term repeat-
ability. Noise levels are assumed small and channel errors
associated with discrete sampling and transmission will be re-
duced with hardware/software processing of the signal.

61

Table 4.2

EDS Instrumentation Characteristics

PARAMETER	SIGNAL SOURCE	OPERATING RANGE	SYSTEM ACCURACY
α	Airframe	-10° - +35°	$\pm$0.10°
PAMB	DDU	10 - 15 PSIA	$\pm$5% of F.S./10 - 15 PSIA
TAMB	DDU	-65 - +120°F	$\pm$2°F/-65 - +120°F
PT2 (DERIVED)	Airframe	1 - 38 PSIA	$\pm$0.5% of F.S./8.5 - 18.8 PSIA
TT2	Engine	-65 - +415°F	$\pm$2°F/-65 - +150°F
N1	Engine	3,000 - 13,000 RPM	$\pm$.2% of PT./3,000 - 12,000 RPM
N2	Engine	6,000 - 15,000 RPM	$\pm$.2% of PT./6,000 - 15,000 RPM
PT6	Engine	0 - 100 PSIA	$\pm$0.5% of F.S./16 - 65 PSIA
FTIT AVE	Engine	0 - 1100°C	$\pm$7°C/0 - 1100°C
AJ	Engine	2.75 - 6.50 Sq. Ft.	$\pm$3% of F.S./2.75 - 6.50 Sq. Ft.
RCVV	Engine	-40 - +4°	$\pm$0.5°/-40 - +4°
TT2.5	Engine	-20 - +315°C	$\pm$4°C/-20 - +191°C
TT3.0	Engine	335 - 685°C	$\pm$2°C/200 - 600°C
PT2.5	Engine	0 - 100 PSIA	$\pm$0.5% of F.S./17 - 60 PSIA
PB	Engine	0 - 600 PSIA	$\pm$0.25% of F.S./100 - 470 PSIA
WFGG	Engine	600 - 14,000 PPH	$\pm$2.0% of F.S./2,400 - 13,400 PPH
MO (DERIVED)	Airframe	0 - 2.6	$\pm$0.5/0 - 2.6
H	Airframe	0 - 80K ft	$\pm$0.2% of F.S./0 - 80 K ft
PLA	Engine	0 - 130°	$\pm$0.5°/0 - 130°

Several detailed digital simulations of the engine are available to develop analytic or generic engine models. The transient simulation program (transient deck) models dynamic engine and control behavior for various conditions of deterioration specified by perturbed values of lumped efficiencies and areas. A detailed steady state performance deck (status deck) is used to match engine performance with an extremely detailed steady state model of the component performance and control laws. This steady state status program is considered an accurate point performance model but does not include nonlinear dynamic effects. The dynamic simulation program has the capability to generate this type of data but the computational overhead can be severe.

4.3 PRELIMINARY MODEL DEVELOPMENT

4.3.1 Generic Baseline Models

A generic baseline model of the F100 was developed in this phase of the program to demonstrate the analytical and numerical procedures involved and to develop the necessary software capability. The EDS sensor set and accuracies were used as the basis for analysis. A data base was developed using the transient deck modeling generic engine performance. A set of measurement equation models was determined. The overall accuracy matching generated engine data was evaluated for a slightly larger flight window than specified for EDS. The conclusion is reached that a generic model can be developed to match the baseline data. Coefficients depend on altitude and speed.

4.3.2 Fault Parameter Selection

Fault parameters were chosen to reflect a "complete" set of component performance parameters. For the rotating machines (e.g. compressors and turbines) the functional relationships are shown by the simplified thermodynamic descriptions of the energy conversion and flow modification processes which occur. For a compressor, these are as follows:

$$T_r = \frac{K}{\eta_c} (P_r^{\gamma - 1/\gamma} - 1) + 1 \tag{4.1}$$

$$\frac{\dot{m}\sqrt{\theta}}{\delta} = A_c f(\frac{N}{\sqrt{\theta}} , P_r, R_N) \tag{4.2}$$

where the isentropic efficiency, η_c, represents the effectiveness of the compressor in raising the gas pressure. The second equation shows the functional relationship between gas flow and rotational speed and pressure. In high power regions, the operating line characteristics will be such that the following is nearly true:

63

$$\frac{\partial f}{\partial P_r} \approx 0 \tag{4.3}$$

In this case, Eqs. (4.1) and (4.2) represent two independent relationships between the four independent variables, $\dot{m}$, T_r, P_r, and N. The two quantities, A_c and η_c can be used to model the changes in component operation resulting in decreased energy conversion efficiency or compression characteristics. Flow continuity and mechanical torque balance are used to determine the unique operating point. Non-ideal flow effects are modeled as pressure loss coefficients (e.g. in a duct) of the form:

$$\frac{\Delta p}{p} = \eta_p \ K_p \ \left(\frac{\dot{m}\sqrt{\theta}}{\delta}\right)^2 \tag{4.4}$$

where K_p models flow-dependent duct losses and η_p can be used to determine changes in this value caused by duct obstructions and radial velocity distribution changes. The torque balance equations do not contain loss effects since small mechanical conversion losses due to bearing friction, etc. can be lumped into the compressor characteristics. Gross changes in these values due to mechanical failures are usually detected by alternate means such as vibration accelerometers.

Component performance can be modeled by effective areas and isentropic (lumped) efficiencies. Flow through the duct, burner, and augmentor volume is modeled by pressure loss coefficients. These equations certainly do not reflect the necessary complexity to accurately model the microscopic processes occurring in the turbofan gas path. For example, mixing and flow in the augmentor volume can be modeled by up to six variable pressure loss terms. However, the performance monitoring procedures assume small variations in overall behavior. Thus, lumped parameter models can be assumed for small enough effects. This assumption must certainly be verified by a detailed analysis

of actual engine performance deterioration. The performance monitoring requirement is not necessary to model microscopic effects, but rather to approximate the behavior of the sensed variables close enough to infer performance changes in one or more components of the system.

The preliminary fault parameters are shown in Table 4.3. They constitute areas and efficiencies in the fan, compressor, high pressure turbine, and low pressure turbine. Flow losses are associated with the duct, burner, and augmentor. These 11 parameters form the initial set of engine descriptors which will be evaluated for possible inclusion in the final algorithm.

Several other variables will also enter the problem as unidentified disturbances whose effect on the accuracy of the estimated parameters is determined, but whose values are assumed random. These variables are distinct from measurement uncertainties in that they cause changes in more than one measured quantity. Thus, in the static algorithm, they produce correlated errors.

Table 4.3

Candidate Fault Parameters

PARAMETER	DEFINITION	RANGE (%)
δA_{FAN}	Fan area change	2.0
$\delta \eta_{FAN}$	Fan efficiency change	2.0
δA_{COMP} ...	Compressor area change	2.0
$\delta \eta_{COMP}$ ...	Compressor efficiency change	2.0
δA_{HT}	High turbine area change	2.0
$\delta \eta_{HT}$	High turbine efficiency change	2.5
δA_{LT}	Low turbine area change	2.0
$\delta \eta_{LT}$	Low turbine efficiency change	2.0
$\delta \eta_{PC}$	Combustor efficiency change	3.0

Three parameters of this type are initially considered important. These are RCVV angle uncertainty, customer bleed and steady state distortion. The RCVV angle is measured in the EDS system. It is scheduled in the control to be a function of corrected rotor speed. However, there can be an uncertainty in this position due to positioning errors. In the monitoring algorithm, control variables are checked against their schedules to determine healthy control performance. For the RCVV actuator, the control input is assumed "on schedule" for the baseline model development and a disturbance term due to off-schedule position added. This term is initially assumed unbiased, but it could be correlated with the past values of RCVV to determine its value more accurately. The customer bleed flow is taken at the compressor discharge to supply to the F-15 environmental control system (ECS). Other bleed air is also taken for turbine cooling and nozzle actuation. There is no accurate measurement of compressor bleed. Bleed is modeled as a random variable with a non-zero mean. The estimated mean is assumed to be the specified nominal flow rate. Using manufacturer data, uncertainty about the mean can be approximated.

4.3.3 Sensor Model Development

Table 4.2 shows the measured variables. It is assumed that thermodynamic properties are determined by two ambient variables (i.e., there is only a small Mach number dependence at subsonic conditions). It is also assumed that the RCVV and CIVV's are on their hardware control schedules and that the customer bleed is at its mean value. In this case, engine behavior can be uniquely specified by four independent quantities. For the preliminary analysis, the set of independent variables specifying engine operation were chosen as T_{T2}, P_{T2}, N_1 and N_2. These variables represent accurately measured quantities except for P_{T2}. The engine face pressure, P_{T2}, is derived from airframe measurement of Mach number and ambient conditions using a detailed inlet

performance model. This "measurement" technique should produce repeatable results which would correlate with an averaged total pressure at the engine face. Uncertainties in this quantity are modeled by distortion values specified as disturbances. The EDS measurement set can be divided into eight dependent and four independent variables. There are 11 fault coefficient variables, three disturbance variables and eight measurement noise variables.

Each of the eight transduced variables is assumed to be sampled from an imperfect instrument with associated instrument fault modeling coefficients. Typically, transducers will exhibit complex systematic error effects. Models are available for typical measurement errors which occur in the static environment. These models are reviewed below for completeness; however, they were not used in the initial evaluation.

Temperature sensors are generally low bandwidth devices that filter high frequency local temperature variations. Outputs which are "averaged" over several circumferential positions from total rakes are typically quite repeatable. Low signal levels can be susceptible to high frequency interference from electro-magnetic components located nearby. This EMI may be dependent on engine power condition. Generally, analog filtering can remove most of this error. Aliasing into the bandpass of the instrument should produce a d.c. error smaller than the transducer repeatability. Some care is necessary in averaging and detrending the inputs to remove these effects. The model for the sensor data can be represented for algorithm development as follows:

$$T_m = T + v + b \qquad (4.5)$$

$$v = N(o,r) \qquad (4.6)$$

The bias term, b, is treated as a long-term calibration drift.

Pressure sensors can exhibit a far more complex behavior due to resonance effects, flow radial distribution shifts, wake

67

effects, temperature changes, etc. Most probes must be temper-
ature corrected either internally or externally. Vibration
sensitivity can be a problem. High frequency aliasing is also
possible without prefiltering. One possible model is as follows:

$$P_m = P(1 + KT) + v + b \tag{4.7}$$

Liquid flow measurements are subject to temperature depen-
dnet inaccuracies, density and velocity profile effects. Most
devices must be carefully calibrated. Inputs must be filtered
and may contain low frequency components due to interactions
with fuel metering dynamics. Models may be assumed to have the
following form:

$$(W_f)_m = f(W_f, \alpha) + b + v \tag{4.8}$$

where α is a manufacturer-specified set of correlations and

$$\frac{\partial f}{\partial W_f} \approx 1 \tag{4.9}$$

Area and RCVV measurements contain bias and hysteresis ef-
fects. Hysteresis can be important in this type of signal. In
this case, the error is not due to the sensor, but to backlash
in linkages. The apparent measurement differs from the actual
value by a function which is dependent on previous position.
These may be written in sampled data form as follows:

$$A(n+1) = \begin{cases} A(n) - h & A_c(n+1) > A(n) + h \\ A(n) & A(n)+h > A_c(n+1) > A(n)-h \\ A(n) + h & A_c(n+1) > A(n) - h \end{cases}$$

$$\tag{4.10}$$

where $A(n)$ and $A_c(n)$ are the actual position and the position
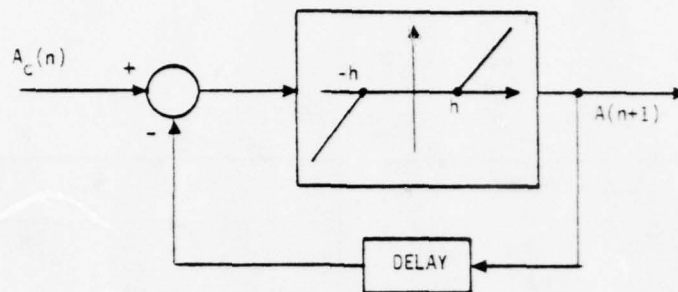with hysteresis. This model is illustrated in Figure 4.1.

Figure 4.1   Hysteresis Model

In the preliminary model development, each of the eight measurements was assumed to have a random, constant bias. The assumption of eight biases increases the uncertainty in the parameter estimates.

4.4   DATA BASE GENERATION AND DATA REDUCTION PROCEDURES

Generic engine data was generated using a detailed engine simulation deck. A large number of operating points were chosen with engine fault parameters set at their undeteriorated values. Fault coefficients and disturbance parameters were perturbed and performance variation calculated at a reduced number of points.

Baseline operating points were chosen to span the envelope of data acquisition in an evenly distributed grid. This data can then be weighted to bias the models toward a more accurate match where large amounts of data will be recorded.

The operating points are chosen in the flight envelope to represent nonstandard conditions. A standard atmosphere profile (Table 4.4) is used as the starting point. Altitude limits determine standard ambient pressures and temperatures. Pressures are assumed constant. Typical hot and cold day temperatures are assumed to vary $\pm 20°F$ of the standard conditions. Isentropic inlet recovery (for subsonic data) is used to construct P_{T2}/T_{T2} curves shown in Figure 4.2. Lines of constant Reynolds index are

Table 4.4
U.S. Standard Atmosphere - 1962

Alt ft	Temp t F	Temp t °R	Temp t °C	Press. P in. Hg	Press. P lb/ft²
0	59.0	518.7	15.0	29.92	2116.
1000	55.4	515.1	13.0	28.86	2041.—
2000	51.9	511.5	11.0	27.82	1968.
3000	48.3	508.0	9.1	26.82	1897.
4000	44.7	504.4	7.1	25.84	1828.
5000	41.2	500.8	5.1	24.90	1761.
6000	37.6	497.3	3.1	23.98	1696.
7000	34.0	493.7	1.1	23.09	1633.
8000	30.5	490.2	-0.8	22.23	1572.
9000	26.9	486.6	-2.8	21.39	1513.
10000	23.3	483.0	-4.8	20.58	1456.
11000	19.8	479.5	-6.8	19.80	1409.
12000	16.2	475.9	-8.8	19.03	1346.
13000	12.7	472.3	-10.7	18.30	1234.
14000	9.1	468.8	-12.7	17.58	1244.
15000	5.5	465.2	-14.7	16.89	1195.
16000	2.0	461.7	-16.7	16.22	1118.
17000	-1.6	458.1	-18.7	15.59	1102.
18000	-5.1	454.5	-20.6	14.95	1058.
19000	-8.7	451.0	-22.6	14.35	1015.
20000	-12.2	447.4	-24.6	13.76	973.3
21000	-15.8	443.9	-26.6	13.20	933.3
22000	-19.4	440.3	-28.5	12.65	894.6
23000	-22.9	436.7	-30.5	12.12	857.3
24000	-26.5	433.2	-32.5	11.61	821.2
25000	-30.1	429.6	-34.5	11.12	786.4
26000	-33.6	426.1	-36.5	10.64	752.8
27000	-37.2	422.5	-38.4	10.18	720.3
28000	-40.7	419.0	-40.4	9.741	689.0
29000	-44.3	415.4	-42.4	9.314	658.8
30000	-47.8	411.8	-44.4	8.903	629.7
31000	-51.4	408.3	-46.3	8.506	601.6
32000	-54.9	404.7	-48.3	8.124	574.6
33000	-58.5	401.2	-50.3	7.756	548.6
34000	-62.1	397.5	-52.3	7.401	523.5
35000	-65.6	394.1	-54.2	7.060	499.4
36000	-69.2	390.5	-56.2	6.732	476.2
37000	-69.7	390.0	-56.5	6.417	453.9
38000	-69.7	390.0	-56.5	6.117	432.7
39000	-69.7	390.0	-56.5	5.831	412.4
40000	-69.7	390.0	-56.5	5.558	393.1
41000	-69.7	390.0	-56.5	5.299	374.8
42000	-69.7	390.0	-56.5	5.051	357.3
43000	-69.7	390.0	-56.5	4.815	340.6
44000	-69.7	390.0	-56.5	4.590	324.6
45000	-69.7	390.0	-56.5	4.375	309.5
46000	-69.7	390.0	-56.5	4.171	295.0
47000	-69.7	390.0	-56.5	3.976	281.2
48000	-69.7	390.0	-56.5	3.790	268.1
49000	-69.7	390.0	-56.5	3.613	255.6
50000	-69.7	390.0	-56.5	3.444	243.6
51000	-69.7	390.0	-56.5	3.284	232.2
52000	-69.7	390.0	-56.5	3.130	221.4
53000	-69.7	390.0	-56.5	2.984	211.1
54000	-69.7	390.0	-56.5	2.845	201.2
55000	-69.7	390.0	-56.5	2.712	191.8
56000	-69.7	390.0	-56.5	2.585	182.9
57000	-69.7	390.0	-56.5	2.465	174.3
58000	-69.7	390.0	-56.5	2.350	166.2
59000	-69.7	390.0	-56.5	2.240	158.4
60000	-69.7	390.0	-56.5	2.135	151.0
61000	-69.7	390.0	-56.5	2.036	144.0
62000	-69.7	390.0	-56.5	1.941	137.3
63000	-69.7	390.0	-56.5	1.850	130.9
64000	-69.7	390.0	-56.5	1.764	124.8
65000	-69.7	390.0	-56.5	1.682	118.9
66000	-69.6	390.1	-56.5	1.603	113.4
67000	-69.1	390.6	-56.1	1.528	108.1
68000	-68.5	391.2	-55.8	1.457	103.1
69000	-68.0	391.7	-55.5	1.390	98.29
70000	-67.4	392.2	-55.2	1.325	93.73

superimposed on these curves. The operating points were chosen equally spaced along lines of constant R_{EI} passing through standard day, altitude-Mach number points which were judged to be operating points in the aircraft flight profile. At each operating point specified by T_{T2}, P_{T2}, a nominal operating Mach number was assumed. Table 4.5 shows the flight points chosen for baseline data generation.

Fuel flow and nozzle area specify the operating point. Nozzle area perturbations of 0.1 sq ft were run at each flight point to assess measurement uncertainty effects.

Five values of fuel flow were chosen at each operating point to match points in the EDS flight envelope (see Table 4.6). The total number of baseline points for this preliminary set of calculations was:
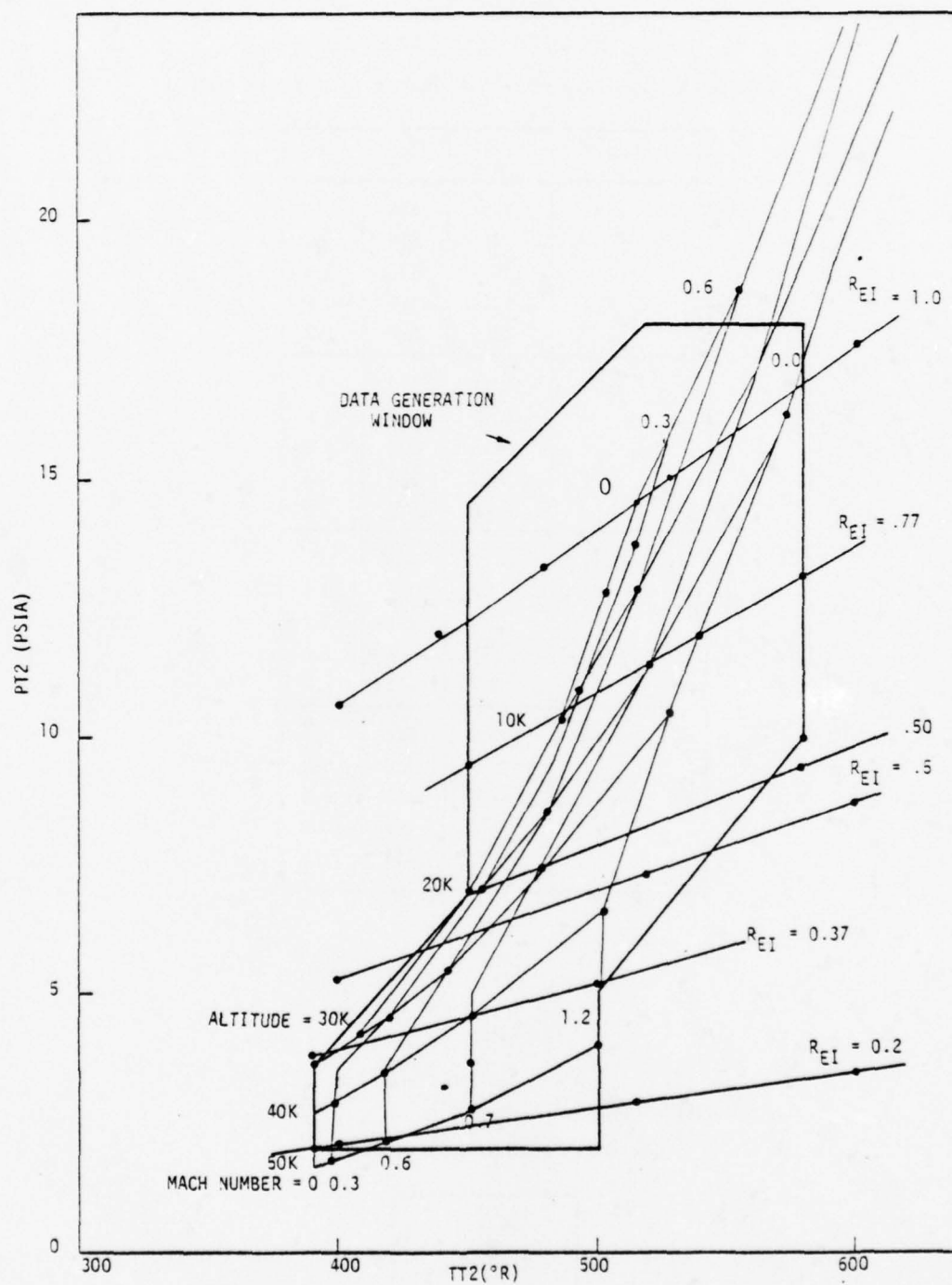
Figure 4.2 Data Generation Points

Table 4.5

P_{T2}-T_{T2} Points at Constant R_{EI}
Chosen for Baseline Data Generation

	P_{T2}	T_{T2}	Mn
R_{EI} = 1.0	13.5	483	0
	14.7	518	0
	15.4	538	0.6
	16.2	560	0.9
	16.9	580	1.2
R_{EI} = 0.77	10.14	474	0
	10.77	498	0.6
	11.4	520	0.9
	12.03	544	1.2
	12.66	567	1.2
R_{EI} = 0.56	7.0	454	0
	7.2	465	0.6
	7.4	478	0.9
	7.8	496	1.0
	8.2	516	1.2
R_{EI} = 0.37	3.8	388	0
	4.07	410	0.3
	4.34	432	0.6
	4.62	453	0.9
	5.00	484	1.2

Table 4.6

Fuel Flow Points
Corrected Fuel Flow ($W_f/\delta_2\sqrt{\theta_2}$)
[% Intermediate Power]

100
95
80
65
50

$$(4 \ R_{EI}) \ x \ (5 \ P_{T2}/T_{T2}) \ x \ (5 \ \text{Fuel Flow}) \ x \ (3 \ A_J) = 300$$

A subset of these baseline points was chosen to create per-
turbational data. Perturbational inputs include positive and
negative variations of a specified amount (see Table 4.3) to
each of the 11 fault variables and variations of bleed and RCVV
position corresponding to two nominal amounts (see Table 4.7)
at a particular flight condition. Flight points were chosen in
"high probability" acquisition windows (Table 4.7). Values of
nozzle area and fuel flow were chosen to be representative of
the flight condition. There were 72 points run with these
inputs.

Stepwise regression was used to fit the simulation data.
Initially, regression terms were chosen as transgenerated poly-
nomial functions of desired variables and nondimensional func-
tional combinations. Table 4.8 lists the functional forms for
the baseline model fits. Accuracy and worst case errors are also
shown.

The fits indicate models with very few terms (< 30) can be
used to fit the engine data closely. The windows chosen for the

Table 4.7

Nonlinear Simulation Points for Perturbed Model Generation

CONDITION	TT2 (°R)			PT2 (PSIA)	MACH NO.	$W_f/\delta_2\sqrt{\theta_2}$ (% INTER-MEDIATE)	DELTA AJ (FT^2)	OFF SCHED-ULE RCVV (DEG)
	HOT	STD	COLD					
0K/0/83	538	518	498	14.7	0	105	-0.1	0
10K/0.6/80	536	516	496	13.9	0.6	102	0.0	±1.0
15K/0.5/70	510	490	470	10.2	0.5	80	0.0	±1.0
10K/0.5/50	514	504	484	11.7	0.5	50	0.0	±1.0
20K/0.9/83	540	520	500	11.4	0.9	108	-.05	0
12K/0.8/70	545	525	505	13.8	0.8	80	0.0	±1.0
8K/0.3/50	524	504	484	12.0	0.3	50	0.0	±1.0
18K/0.8/83	548	528	508	12.4	0.8	110	+0.5	0
0K/0/70	538	518	498	14.7	0.0	105	0.0	1.0
5K/0.2/60	526	506	486	12.7	0.2	63	0.0	1.0

Table 4.8

Baseline Model Equations

FAN STREAM VARIABLES

MEASURE-MENT	δ_2	θ_2	W_f	N_1	N_2	A_J	$N_1^3\theta_2$	$N_1^2\theta_2^{-\frac{1}{2}}\delta_2$	$N_1^3\theta_2^{-\frac{1}{2}}$	$\delta_{2.5}^2\theta_2^2\delta_{2.5}^{-2}$	$N_1^3\delta_2 e^{-1}$	$N_2^2\delta_{2.5}^{-\frac{1}{2}}$	$N_2^2\theta_2^3\delta_{2.5}^{-\frac{1}{2}}$	$A_J^2\delta_2\theta_2^2$	$\delta_{2.5}$	$A_J^3\delta_2$	CONST.	STD. ERROR	UNITS
N_1	-0.122	0	0.015	0	0	0	0	0.	0	0	0	0.496	0.129	0.118			0.096	1%	% RPM
PT2.5C	0	1.317	0	1.098	0	-1.46	0	4.87	0	0	-2.10	0	0	0			0.377	1%	ATM
TT2.5C	0	0	0	0	0.569	0	-0.493	0	0.233	0.016	0	0	0	0			-0.465	1.5%	% STD
PT7M	0	0	0	0	0	0	0	0.836	0	0	-0.271	0	0	0	-0.900	-0.443	0	0.3%	ATM

CORE STREAM VARIABLES

MEASURE-MENT	$\delta_{2.5}$	$\theta_{2.5}$	$(W_f/\delta_{2.5})\theta_{2.5}$	$(W_f/\delta_{2.5})\theta_{2.5}^{\frac{1}{4}}$	$(W_f/\delta_{2.5})^3$	$N_2^3\theta_{2.5}$	$N_2\theta_{2.5}^3$	$A_J\delta_{2.5}^{\frac{1}{2}}$	$\delta_{2.5}^3$	$(W_f/\delta_{2.5})^2$	$N_2^2\delta_{2.5}^2\delta_{2.5}^{-1}$	N_2	CONST.	STD. ERROR	UNITS
N_2	0.008	0.448	-1.27	1.91	1.247	0	0	0	0	0	0	0	0.421	0.01%	% RPM
TT3	0	0	0	0	0	-0.064	1.964	0.0998	0	0	0	0	-.121	0.15%	% STD
PT4	5.58	0	0	0	0	0	0	0	-0.266	20.0	1.256	0	1.92	0.01%	ATM
TT45	-0.056	-1.95	0	0	4.07	-0.089	0	0	0	0	0	3.19	-1.30	0.15%	% STD

data base are larger than expected for EDS performance and trend acquisition. Alternate algorithms utilizing globally optimal regression models were available as well as more sophisticated transgeneration procedures. However, since the transient deck represents a slightly different definition of the performance than the status deck, further investigation of improvement of the model structure will be pursued in the next contract phase.

The baseline models shown in Table 4.8 were subtracted from the perturbed operating data points. These residuals were then regressed for models of the following form:

$$\Delta y = \theta g_1(x,u) \qquad\qquad (4.11)$$

where $g_1(x,u)$ represents polynomial functions of the corrected and uncorrected states and controls. A subset regression technique is used to choose only those variables which affect the perturbations according to the model equation. Table 4.9 shows an example of the variable fault coefficient regression for the compressor efficiency effects on the fan corestream measurements. This procedure is repeated for each fault parameter to determine the full matrix of valuable fault coefficients, $g_{\theta x}$.

Table 4.9

Example of Generation of Variable Fault
Coefficients for Compressor Efficiency
Using Core Stream Variables

$$N_2 - N_{2_0} = \eta_c[a_{11} + a_{12}\,\theta_{2.5} + a_{13}\,N_2^2 + a_{14}\,W_f/\sqrt{\theta_{2.5}}]$$

$$\pi 3 - \pi 3_0 = \eta_c[a_{21} + a_{22}\,N_2^2 + a_{23}\,W_f/\sqrt{\theta_{2.5}}]$$

$$PT4 - PT4_0 = \eta_c[a_{31} + a_{32}\,\theta_{2.5} + a_{33}\,N_2^2 + a_{34}\,W_f/\sqrt{\theta_{2.5}}]$$

$$\pi 45 - \pi 45_0 = \eta_c[a_{41}\,N_2^3]$$

75

Full development of an estimation model will be undertaken in the second phase of the program. The status deck will be utilized to generate data for regression within the EDS flight envelope.

4.5 ALGORITHM OUTPUTS - ENGINE HEALTH ASSESSMENT

Once a model has been established, parameter estimates must be related to maintenance and trend decisions. Specific causative phenomena, viz. foreign object damage, seal leakage, fouling, etc., will affect these parameter values. A correlation between parameter changes and specific deterioration mechanisms will be aided by AMT type testing as well as the EDS flight test program itself.

The user-directed output of the identification procedure must consist of information with which maintenance personnel and logistic support can confidently make repair and overhaul decisions. It is specifically in this area that advanced monitoring procedures will have their most substantial payoff.

Previous fault isolation systems have relied on threshold detection of parameter values. When a failure occurred, the threshold exceedances were compared to patterns for typical fault situations. Most easily replaced items, e.g. sensors, are initially changed in an attempt to correct the problem. In a sense, the threshold values were utilized to filter out uncertainties in parameter estimates due to noisy data input.

The performance monitoring algorithm utilized for fault diagnosis and isolation with the EDS data will primarily monitor shifts in fault parameters and instrument bias estimates to detect changes in sensor accuracy or performance shifts.

The algorithm output provides a state estimate which is made by "smoothing" the noisy measurements with the modeled performance. The measurements of control actuator values and control input values can be used in an "inverse" control model

to accurately assess the performance of the hydromechanical and electronic fuel control on the F100. It is possible to diagnose the control to the component part using this procedure.

A hypothetical example of this procedure is given below. A set of data is processed indicating that the RCVVs have shifted from the hardware schedules and that the engine is running at a different operating condition for a specific power point. This information is derived from the accurate analytic model which represents the operation of the engine with the most current deterioration parameters and a model of the hydromechanical fuel control which has been identified to match previous flight data. Since the anomalous behavior is common to both the fuel flow output and RCVV output, the RCVV actuation system is eliminated along with specific internal hydromechanical governor failure. The remaining two candidates are the hydromechanical speed and temperature sensors and plumbing of the fuel signal pressures into the hydromechanical control.

The most important diagnostic output of the performance monitoring algorithm is an assessment of engine health relative to long term aging and normal deterioration. This information must be presented to the maintenance personnel as a condensed figure representing the impact on routine maintenance activities. Long term analysis and calculation of population statistics and trends are performed at a remote site. This processing may utilize flight data which has been reduced to parameter and variance estimates at the base level. This procedure results in a significant reduction of data transfer, storage, and manipulation overhead.

Maintenance area decisions can be summarized as the determination to remove an aircraft from the flight line, to attempt engine control trim, and to remove an engine from an aircraft for further maintenance. It is most economical to maintain only those engines that require service and to be able to schedule maintenance to keep work level constant and part movement uniform.

The decision to remove an aircraft from the flight line can be made if the performance of the engines is significantly degraded relative to normal operating standards. The precise level of degradation allowed will be a function of the status of the remaining engines and the present workload. It is desirable to formulate a single figure-of-merit which can be used to evaluate an engine's present performance relative to the other aircraft engines (rather than to itself when it was new).

One such figure of merit has been proposed as the remaining turbine temperature trim margin in the control. Assuming that various engine components have not failed or are not damaged, the level of engine degradation can be assessed by the overall thermal efficiency of the system in converting fuel to thrust. This figure does not reflect module-directed phenomena. However, this number can be used to schedule engine trim activities and maintenance shop scheduling. Further breakdown to module status is appropriate to the intermediate maintenance shop which must overhaul degraded engines.

The engine turbine temperature margin must be viewed as a combination of overall performance variables (i.e. as an overall efficiency) which assesses the engine status relative to the minimum acceptable standard. This figure is not necessarily related to a particular build of engine and control which is trimmed on a particular day.

A "standard" FTIT margin, ΔTT_o, can be defined as the difference between the running FTIT and the FTIT limit as specified for the nominal control schedule at P_{STD}, T_{STD} (1 ATM, 518°R), zero air speed conditions at intermediate power when the engine is turbine-temperature limited. This margin will represent the mean value of measured temperature margin for a population of engines and controls of the same degraded status which are trimmed at sea level standard conditions.

Practically, given the engine fault parameters, the ΔTT_0 for that engine can be estimated directly from the baseline models as follows:

$$PT7M_0 = f_1(TT2 = 518°R, PT2 = 1ATM, \delta\theta, N_1, N_2)$$

$$TT45 = f_2(TT2 = 518°R, PT2 = 1ATM, \delta\theta, N_1, N_2)$$

$$N_1 = f(N_2, TT2 = 518°R)$$

i.e., the value of PT7M (EPR) is specified by the trim curves, N_1 is a specified control function of N_2 and T_{T2}, the geometry is on schedule and the bleeds are closed. These conditions can be used to solve for the unique standard operating point solution for $\hat{TT}45$ and

$$\Delta\hat{TT}_0 = TT45_{MAX}(TT2 = 518°R) - \hat{TT}45$$

This value is an estimate of the actual margin for the engine if trim is performed at these standard conditions. Variance information is available from the parameter estimates and model sensitivity calculations.

The standard margin, ΔTT_0, is utilized to measure the "closeness" to maximum overall degradation $(\Delta TT_0 = 0)$ and the relative degradation between two engines $[(\Delta TT_0)_1 \gtrless (\Delta TT_0)_2]$. This information may be monitored and maintenance activities scheduled according to probable predicted status using this method.

4.6 REAL-TIME DATA ACQUISITION TECHNIQUES

Several methods for processing sequential measurements are presented. These reduce uncertainty due to measurement noise, slow trends and sudden changes during recording. A typical data

79

acquisition procedure is to record only when the system has
assumed a steady state condition for several minutes. When this
occurs, measurements are taken with synchronous or asynchronous
scans of the sensors and the scans are averaged. In this way,
the standard deviation of the noise can be reduced by a factor of
nearly $\sqrt{N}$, where N is the number of scans. This procedure
leads to poor results when the system is undergoing a small
transient as shown in Figure 4.3. Thus, the performance data
windows are restricted to regions of the flight envelope where
the steady state requirements can be met without impacting the
mission. It is possible that an entire mission will be flown
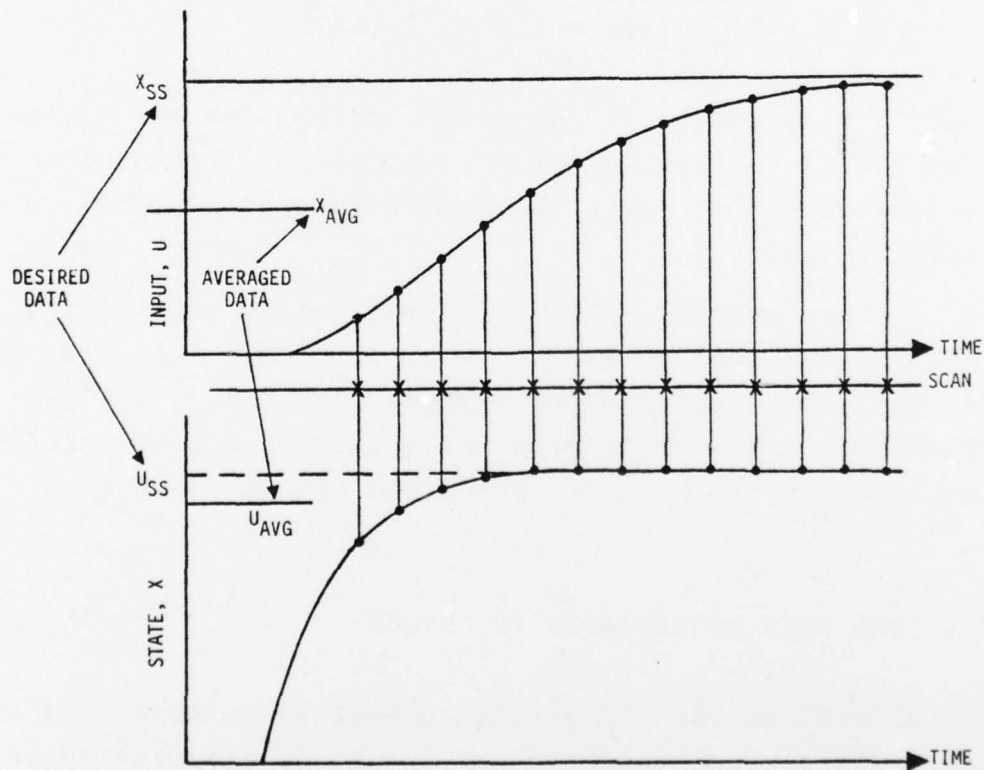without any performance data being taken.

Figure 4.3 Effect of Average Scan in Nonequilibrium
Condition Versus Estimation Procedure

Several single-channel processing procedures are commonly available for accurate data acquisition. The first method uses a variance estimate as a recording threshold. Basically, data is taken when the previous N scans have been acceptably constant. The average of the N last measurements is calculated as follows:

$$\overline{X}_j(i) = \frac{1}{N} \sum_{i=1}^{N} X_j(i) \qquad j=1,\ldots,m$$

where $X_j(i)$ is the jth measurement at time i. The sample variance is calculated as follows:

$$\sigma_j^2(i) = \frac{1}{N-1} \sum_{i=1}^{N} (X_j(i) - \overline{X}_j(i))^2$$

and a weighted sum of the variances is used as a threshold:

$$T(i) = \sum_{j=1}^{m} W_j \, \sigma_j^2(i)$$

The mean of the data is recorded at time i when

$$T(i) < T_{min}$$

where T_{min} can be chosen small enough to assure that the sample mean is close to the real mean to high probability. Figure 4.4 illustrates this concept.

The above procedure requires N storate locations and mN multiplications per step. A more easily implementable procedure is developed as follows. This procedure is commonly referred to as low pass or exponential filtering. At time i,

$$\overline{X}(i+1) = \overline{X}(i) + \frac{1}{N} (X(i+1) - X(i+1-N))$$

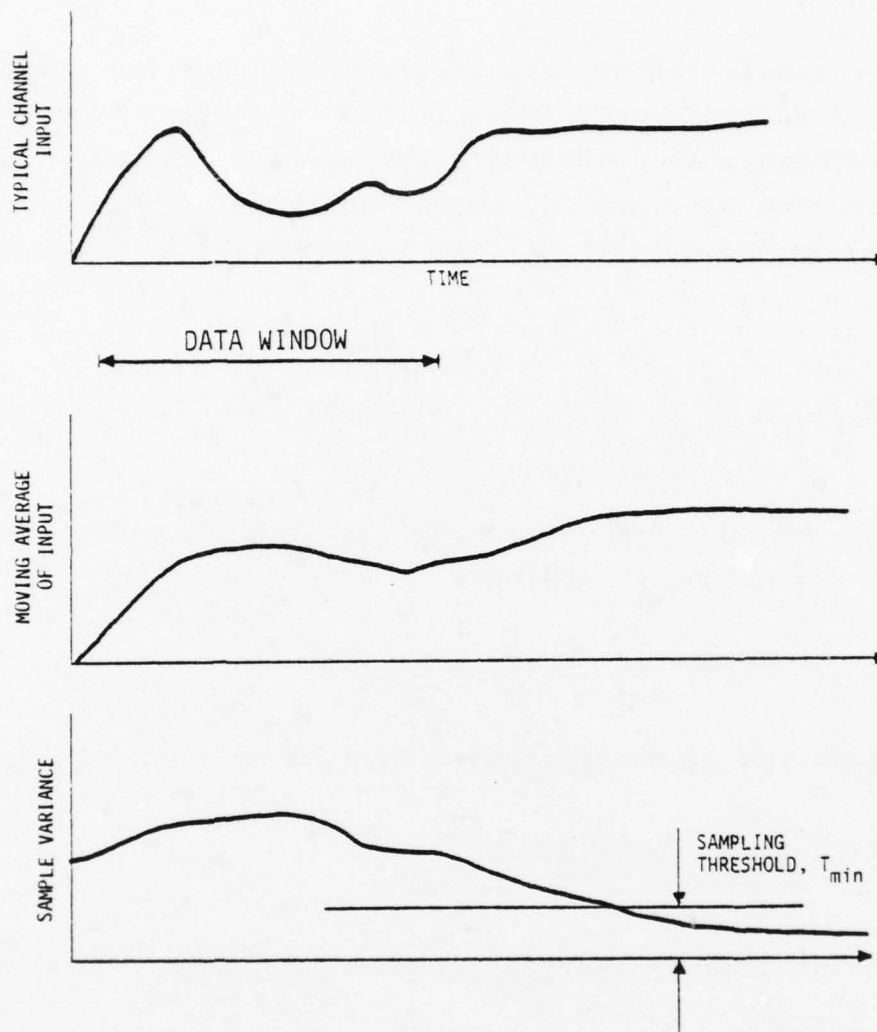If the Nth delayed measurement, $X(i+1-N)$, has not been stored, the best estimate is

Figure 4.4   Data Acquisition Logic

$$\overline{X}(i) \approx X(i+1-N)$$

and the formula reduces to the following

$$\hat{\overline{X}}_j(i+1) = \frac{N-1}{N} \hat{\overline{X}}_j(i) + \frac{1}{N+1} X_j(i+1) \quad j=1,\ldots,m$$

which requires no more storage locations than averaging. Using a similar argument, the sample variance is

$$\hat{\sigma}_j(i+1) = \frac{N-1}{N-2} \hat{\sigma}_j(k) + \frac{1}{N-1} (X_j(i+1) - \hat{X}_j(i+1))^2 \quad j=1,\ldots,m$$

The same threshold detection scheme can be applied with little loss of precision.

A further implementation tradeoff can be evaluated considering the error statistics of the above filter. Consider measuring a constant value with white, Gaussian errors additionally superimposed:

$$y(n) = x(n) + v(n)$$

where

$$v = N(0,R)$$

and

$$x(n+1) = x(n)$$

The optimal sequential filter for this system can be written as follows:

$$\hat{x}(n+1) = \hat{x}(n) + K(n) [y(n+1) - \hat{x}(n)]$$

$$K(n) = \frac{S(n)}{R+S(n)}$$

$$S(n+1) = [1-K(n)]^2 S(n) + K(n)^2 R$$

where

$$S(n) = cov(\hat{x} - x)$$

If it is assumed that no a priori information exists for x,

$$S(0) = \infty$$

then

$$K(n) = \frac{1}{n+1}$$

$$S(n) = \frac{R}{n}$$

i.e. the optimal Kalman filter reduces to the averaging algorithm described above. The tradeoffs associated between calculating the sequentially varying gain, $K(n)$, and a constant value can be determined by analyzing the a posteriori error covariance $S(n+1)$ for these systems. These figures are shown in Figure 4.5. This plot indicates that the filter statistics reach stationarity more quickly at higher gains, but the overall performance is degraded. Acceptable performance can be realized with constant gains. As an example, consider the situations presented in Table 4.10 where actual differences in optimal and suboptimal filter behavior are shown to be small. This permits a simplified implementation of the data acquisition algorithm.

Time-varying data can be assumed to have a constant drift. In this case, the measurement is assumed to be taken at equal time increments, Δ, and have the following form:

$$X(t) = X(0) + Bt$$

Using the N scans, the best estimate of the base value can be written as follows:
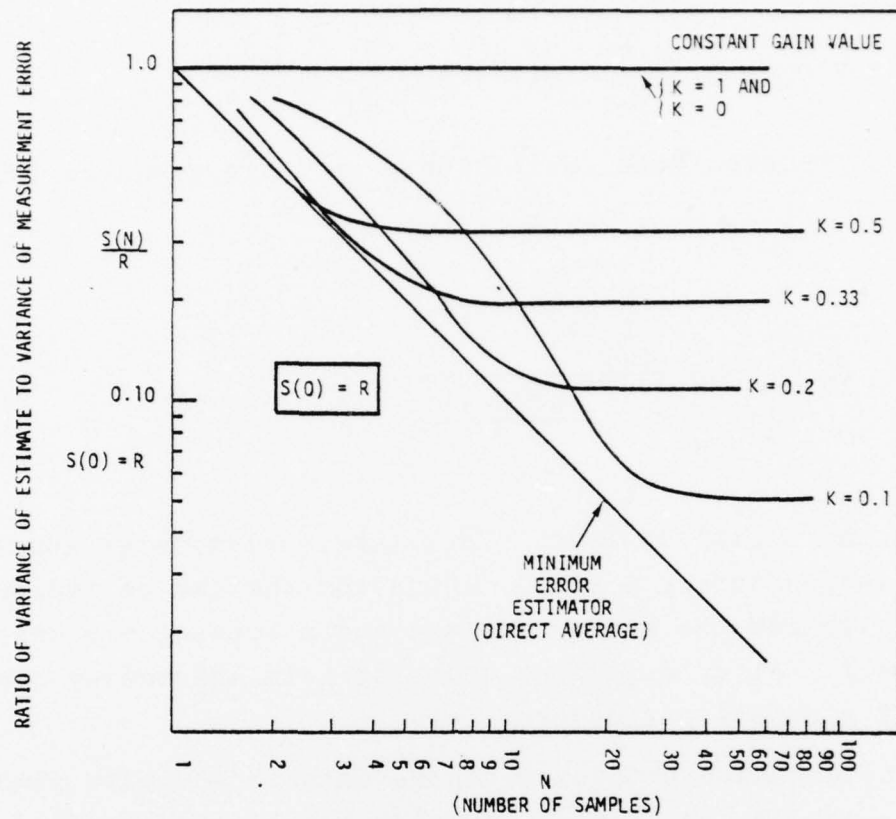
84

Figure 4.5   Mean Square Error Reduction using
Time Varying and Steady Gains

Table 4.10

Comparison Estimation Errors for Optimal
Varying Gain and Constant Gain

N (NO. OF SAMPLES)	K	S(N)/R OPTIMAL	OPTIMAL FIXED GAIN
5	0.29	0.20	0.228
10	0.18	0.10	0.124
30	0.02	0.02	0.03

$$\hat{X}(0) = K_1 \sum_{i=1}^{N} X(i) + K_2 \sum_{i=1}^{N} iX(i)$$

where the precalculated coefficient, K_1, is given as follows:

$$K_1 = \frac{\sum_{j=1}^{N} i^2}{\left(N \sum_{i=1}^{N} i^2\right) - \frac{N^2(N+1)^2}{2}}$$

and K_2 has a similar form. This scheme eliminates constant time variation during a scan. The algorithm can be implemented sequentially and the memory storage and processor overhead are quite small. Also, a similar constant gain assumption can be used with a modest performance loss.

An alternative procedure can be used to estimate final values in the engine when the process has been identified as a slow exponential decay to equilibrium. The time constants may be estimated from engine test data and the dynamics can be written as follows:

$$\dot{x} = F(x - x_f)$$

or solving for the discrete time solution:

$$x(n+1) = \Phi x(n) + (I - \Phi) x_f$$

where

$$\Phi = \exp(F \cdot \Delta T)$$

$$x(n+1) = x(n\Delta T + \Delta T)$$

$$x_f = x(\infty)$$

This equation can be solved for x_f:

$$x_f(n) = x(n) + (\Phi^{-1} - I) \, \Delta x(n)$$

where

$$\Delta x(n) = x(n+1) - x(n)$$

The final value can be sequentially estimated for this solution as follows:

$$\hat{x}_f(n+1) = \hat{x}_f(n) + K(x_f(n) - \hat{x}_f(n))$$

where the gain vector K is most easily chosen as a particular constant Kalman filter gain or an observer design.

4.7 SUMMARY

A preliminary study has been described which assesses the feasibility of developing generic engine models for the F100 turbofan. The models are designed to operate on flight-acquired data from a currently developing avionics system, the EDS. Engine operating data is generated using a nonlinear digital simulation for the EDS performance data acquisition window. Models using polynomial terms are derived from the baseline data. Several fault coefficients are calculated which are explicit functions of the operating point. A full set of generic engine baseline models and variable fault coefficient equations can be used as the foundation of the fault parameter estimation algorithms presented in Section III. The results indicate that the engine operating data and off-nominal responses can be matched accurately with a set of equations requiring only a small amount of para- meter storage and calculation capability.

SECTION V

SUMMARY AND CONCLUSIONS

The problem of engine fault monitoring is difficult to define because of the many mathematical modeling, physical hardware and software considerations, and test and evaluation aspects, which must be evoked. Figure 5.1 illustrates some of the more significant aspects. The overall scope of this program was to bound the engine fault monitoring problem by selecting a particular subset of these various requirements, formulating specific fault isolation criteria from a general diagnostic theoretical framework, and subsequently investigate the development of a software system to achieve a practical diagnostic tool.

The particular diagnostic application selected for this program was that of thermodynamic cycle monitoring (TCM). Vibration and accessory monitoring are not included, for example. Within the TCM scope, however, considerations of maintenance and trim procedures, sensor fault detection, and snapshot recording can be integrated to provide an operational diagnostic procedure.

The objective of the overall program is to provide a totally self-contained, well-documented, and validated gas path diagnostic system for utilization on advanced installed engine data. Specific application is to the Air Force F-15/F100 system, data obtained from the Engine Diagnostic System (EDS) program. This EDS program is the most advanced in-flight monitoring opportunity to integrate a unique set of typical data into this proposed software program. The overall program can produce a software code which is compatible with the EDS system.

This aspect of fault detection and isolation is particularly important to the Navy and the Air Force because of the significant improvements in aircraft availability, reduction in engine maintenance costs, and increased safety of flight which results from the ability to accurately diagnose engine operational
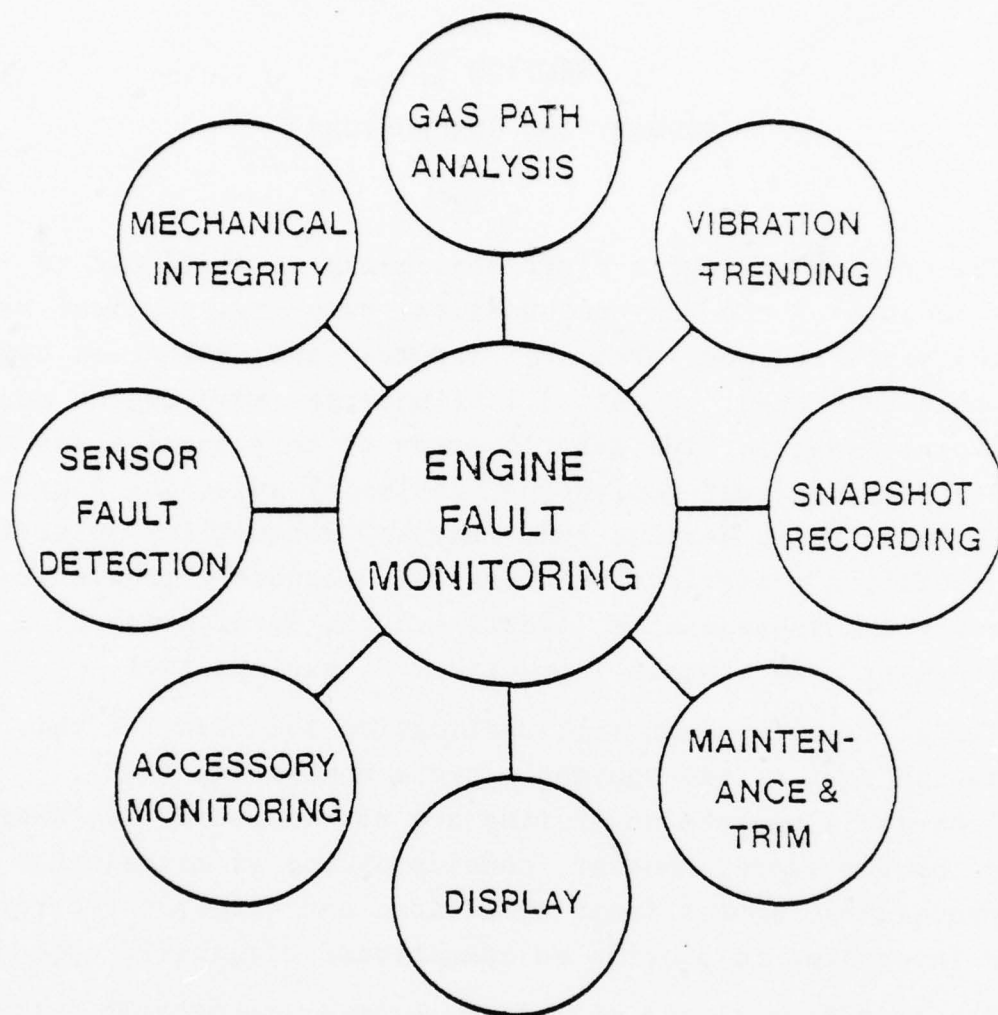
Figure 5.1   Requirements of Engine Fault Monitoring

characteristics before severe failures.   Such benefits have
already been demonstrated in the Navy in-flight Engine Condition
Monitoring System (IECMS) now being tested on TF41 engines in
the VSD A-7E aircraft.   Future aircraft systems which will
incorporate these concepts are the F404 turbofan engines in the
Navy's F-18 fighter, and the Air Force's F100 turbofan engine
used on the F-15 and F-16.   Beyond these present aircraft, it is
anticipated that future advanced cycle engines will require even
more sophisticated diagnosis systems as the complexity required
for higher performance increases.

REFERENCES

1. Gupta, N.K. and Hall, W.E., "System Identification Methodology for Fault Detection and Isolation in Dynamical Systems," Engineering Technical Report for ONR under contract, Nov. 1977.

2. Barclay, B.A., "FADEC Preliminary Design Overview for Variable Cycle Engine Control," AIAA/SAE No. 77-837, 1977.

3. Taylor, H.N., "Maintenance Trends for New Air Transport Power Plants," SAE No. 700326, 1970.

4. Doran, P.D., "Some Historical Highlights of Turbine Engine Condition Monitoring using Flight Data," SAE No. 700314, 1970.

5. Sallee, G.P., Kruckenberg, H.D., and Toomey, E.H., "Analysis of Turbofan Engine Performance Deterioration and Proposed Follow-On Tests," NASA CR-135769, 1975.

6. Smetana, F.O., "Turbojet Engine Gas Path Analysis," AGARD Conf. Proc. No. 165 on Diagnostics and Engine Condition Monitoring, April 1974.

7. Vermeullen, H., "KSSU Aids Engine Analysis," AGARD Conf. Proc. No. 165 on Diagnostics and Engine Condition Monitoring, April 1974.

8. Mucklow, P.A., "Engine Data Recording on a Phantom Aircraft - Results Obtained to Date," AGARD Conf. Proc. No. 165 on Diagnostics and Engine Condition Monitoring, April 1974.

9. Dahl, G., "Some Experience in Engine Troubleshooting with In-Flight Data, Recorded in the F-104G with the Leads-200," AGARD Conf. Proc. No. 165 on Diagnostics and Engine Condition Monitoring, April 1974.

10. Van Cleve, G.C., "In-Flight Engine Condition Monitoring System," Instrumentation for Airbreathing Propulsion, The MIT Press, Cambridge, Mass., and London, England, 1974.

11. Downing, N.L., "Control System and Condition Monitoring Integration," AIAA No. 75-1179, 1975.

12. Belrose, T.C., "Testing of Propulsion System Diagnostic Equipment," AIAA/SAE 13th Joint Propulsion Conf., Orlando, Florida, AIAA Paper No. 77-895, 1977.

13. Belrose, T.C., "Automatic Inspection, Diagnostic and Prognostic System (AIDAPS), An Automatic Maintenance Tool for Helicopters," AGARD Conf. Proc. No. 165 on Diagnostics and Engine Condition Monitoring, April 1974.

14. Reis, J.J., and Groves, R.C., "Helicopter Gearbox Failure Prognosis," AIAA Paper No. 77-897, 1977.

15. Krupa, W.R., and Hamiltron, K.R., "An Advanced Diagnostic Engine Monitoring System Approach," AGARD Conf. Proc. No. 165 on Diagnostics and Engine Condition Monitoring, April 1974.

16. Kruckenberg, H.D., "Design and Testing of the American Airlines Prototype," American Airlines, Tulsa, Okla., Vol. 9, No. 4, 1972.

17. Arnold, B.R. and Gast, J.R., "A Cooperative Airline Program to Evaluate Engine Parts Aging Effects on a Current Turbofan Engine Model," SAE Paper No. 700329, April 1970.

18. Barschodorff, D., "Theory of Periodic Turbomachine Noise and Determination of Blade Damage from Noise Spectrum Measurements," AGARD Conf. Proc. No. 165 on Diagnostics and Engine Condition Monitoring, April 1974.

19. McDonnel Aircraft Company, Pratt & Whitney Aircraft and General Dynamics Corporation," F100 Engine Diagnostic System Hardware and Software Definition Phase," MDC A4270, 1976.

20. R & M Subcommittee Air Transport Association, "Airline/ Manufacturer Maintenance Program Planning Document," MSG-2, 1970.

21. Taylor, W.R. and Ogg, J.S., "Accelerated Mission Testing of Gas Turbine Engines," SAE paper AIAA No. 77-992, 1977.

22. Sibley, R.K., "Engine Condition Monitoring as a Part of the Propulsion Management Concept," Instrumentation for Airbreathing Propulsion, The MIT Press, Cambridge, Mass. and London, England, 1974.

23. Swindlehurst, P.W., "A Military Operator's View of Aero-Engine Low Cycle Fatigue Monitoring," AGARD Conf. Proc. No. 165 on Diagnostics and Engine Condition Monitoring, April 1974.

24. Skala, G.F., "The In-Line Oil Monitor and Its Role in Engine Condition Monitoring," Instrumentation for Airbreathing Propulsion, The MIT Press, Cambridge, Mass., and London, England, 1974.

25. Van Gelder, F.M., "Turbine Engine Diagnostic Development," Naval Air Propulsion Test Center, Trenton, N.J., AD-776, 338, 1974.

26. Couch, R.P., Rossback, D.R. and Burgess, R.W., Jr., "Sensing Incipient Engine Failure with Electrostatic Probes," Instrumentation for Airbreathing Propulsion, The MIT Press, Cambridge, Mass., and London, England, 1974.

27. Cockshutt, E.P., "Equilibrium Performance Analysis of Gas Turbine Engines Using Influence Coefficient Techniques," National Research Council of Canada, 1967.

28. Urban, L.A., "Gas Path Analysis Applied to Turbine Engine Condition Monitoring," Hamilton Standard Division of United Aircraft, Windsor Locks, Conn., Vol. 10, No. 7, 1973.

29. Staples, L.J. and Saravanamuttoo, J.I.J., "An Engine Analyzer Program for Helicopter Turboshaft Powerplants," AGARD Conf. Proc. No. 165 on Diagnostics and Engine Condition Monitoring, April 1974.

30. Kos, J.M., "Multiple Fault Gas Path Analysis Applied to a Twin Spool, Mixed Flow, Variable Geometry, Turbofan Engine," Naval Air Propulsion Test Center, 1975.

31. Urban, L.A., "Gas Path Analysis Applied to Turbine Engine Condition Monitoring," J. Aircraft, Vol. 10, No. 7, 1973.

32. Kos, J.M., "Multiple Fault Gas Path Analysis Applied to TF-30-P-408 Engine Data," AD-785-265, 1974.

33. Cockshutt, E.P., "Gas Turbine Cycle Calculations: Differential Methods in the Analysis of Equilibrium Operation," National Research Council of Canada, Vol. 1, No. 1, 1968.

34. Barbot, A., "Diagnostic De L'etat de Fonctionnement D'un Moteur par Modelisation," AGARD Conf. Proc. No. 165 on Diagnostics and Engine Condition Monitoring, 1974.

35. Andrennucci, M. and Lazzerette, R., "Problems in Fault Diagnostics and Prognostics for Engine Condition Monitoring," AGARD Conf. Proc. No. 165 on Diagnostics and Engine Condition Monitoring, April 1974.

36. Caspi, P., Rault, A., and Esmenjaud, O., "Etude D'un Systeme de Maintenance Preventive Personnalisee par Diagnostic et Pronostic de Pannes. Application aux Reacteur," AGARD Conf. Proc. No. 165 on Diagnostics and Engine Condition Monitoring, April 1974.

37. Wells, W.R., "Failure Detection of Aircraft Engine Output Sensors via Bayesian Hypothesis Testing," AIAA/SAE No. 77-838, 1977.

38. Otto, E.W. and Taylor, B.L., "Dynamics of a Turbojet Engine Considered as a Quasi-Static System," 1950.

39. Urban, L.A., "Parameter Selection for Multiple Fault Diagnostics of Gas Turbine Engines," AGARD Conf. Proc. No. 165 on Diagnostics and Engine Condition Monitoring, April 1974.

40. Honeywell, "Sensor Reduction with Fault-Tolerant Digital Flight Control," AFFDL-TR-77-25, Air Force Flight Dynamics Laboratory, 1977.

41. Meador, B.M. and Nemecek, J.F., "Advanced Airborne System for Maintenance Monitoring," SAE No. 730955, 1973.

42. Gravelle, J.A., "A New Jet Engine Thrust Measuring System: An Advancement in Flight Test Engineering," Soc. of Flight Engineers, Fifth Annual Proc., 1974.

43. Urban, L.A., "Gas Turbine Engine Parameter Interrelationships," United Aircraft Corp., 1967.

44. Mullter, B. and Bott, F., "Experience with F-104G FDRS Evaluation with Respect to Engine Diagnostics," AGARD Conf. Proc. No. 165 on Diagnostics and Engine Condition Monitoring, April 1974.

45. Snowball, H.M., "Engine Aids and the Metrologist Syndrome," Instrumentation for Airbreathing Propulsion, The MIT Press, Cambridge, Mass., and London, England, 1974.

46. Debs, A.S., "Estimation of Steady-State Power System Model Parameters," IEEE Trans. on Power Systems, 1973.

47. Gupta, N. and Hall, W.E., "Methods for Real-Time Identification of Vehicle Parameters," Technical Report No. 4, Office of Naval Research, February 1975.

48. Willsky, A.S., "A Survey of Design Methods for Failure Detection in Dynamic Systems," 1976.

49. Mehra, R.K., "Adaptive Kalman Filtering," IEEE Transactions on Automatic Control, AC15, No. 2, April 1970.